CHAPTER 18

BEAM CLEANING AND COLLIMATION SYSTEM

18.1 INTRODUCTION

Each of the two LHC rings will handle a stored beam energy of up to 350 MJ (3×10^{14} p at 7 TeV), two orders of magnitude beyond the achievements in the Tevatron or HERA [1]. Comparing transverse energy densities, LHC advances the state of the art by even three orders of magnitude, from 1 MJ/mm^2 to 1 GJ/mm^2. This makes the LHC beams highly destructive. At the same time the superconducting magnets in the LHC would quench at 7 TeV if small amounts of energy (on the level of 30 mJ/cm^{-3}, induced by a local transient loss of 4×10^7 protons) are deposited into the superconducting magnet coils [2].

Any significant beam loss into the cold aperture must therefore be avoided. However, beam losses cannot be completely suppressed. A so-called "primary beam halo" will continuously be filled by various beam dynamics processes and the beam current lifetime will be finite [3]. The handling of the high intensity LHC beams and the associated high loss rates of protons requires a powerful collimation system with the following functionality:

1. Efficient cleaning of the beam halo during the full LHC beam cycle, such that beam-induced quenches of the super-conducting magnets are avoided during routine operation.
2. Minimization of halo-induced backgrounds in the particle physics experiments.
3. Passive protection of the machine aperture against abnormal beam loss. Beam loss monitors at the collimators detect any unusually high loss rates and generate a beam abort trigger.
4. Scraping of beam tails and diagnostics of halo population.
5. Abort gap cleaning in order to avoid spurious quenches after normal beam dumps.

The collimators must be sufficiently robust to fulfill these tasks without being damaged both during normal and abnormal operational conditions.

Design work on an appropriate LHC collimation system started in 1990 [4]. The design evolved significantly over the years [5, 6, 7, 8, 9, 10, 11, 12, 13], reflecting both the difficulties to meet the LHC requirements and the challenge of advancing the state of the art in beam cleaning and collimation into a new regime. The latest critical revision of the LHC collimation system started in 2002 [14]. The final collimation design for the LHC has been fixed but not all details have been worked out. This chapter summarizes the design status in January 2004.

18.2 DESIGN GOALS

Any possible hardware solution for the collimators can only resist a small fraction of the LHC beam [14, 15]. The maximum beam load that is expected on the collimators must be estimated in order to make an appropriate design. Experience from operating accelerators shows that beam losses are always higher than the theoretical optimum. Real-world beam losses are driven by imperfections, operational problems, unexpected beam physics processes, technical components operating out of specification, human errors and failures of equipment. This section summarizes the assumed beam load on the collimators. Based on these estimates the required cleaning efficiency is derived and some design principles for the layout of the collimation system are summarized. The collimation design is here described for proton-proton operation of the LHC. Specific design constraints exist for ions and are discussed in Chapter 21.

18.2.1 Specification of maximum collimator beam load

Beam impact at the collimators is divided into normal and abnormal processes [16, 17, 13]. Normal proton losses can occur due to beam dynamics (particle diffusion [3], scattering processes, instabilities) or operational variations (orbit, tune, chromaticity changes during ramp [18], squeeze, collision). These losses must

Table 18.1: Specified minimum beam lifetimes τ, their duration T, the proton loss rate R_{loss}, and maximum power deposition P_{loss} in the cleaning insertion.

Mode	T [s]	τ [h]	R_{loss} [p/s]	P_{loss} [kW]
Injection	cont	1.0	0.8×10^{11}	6
	10	0.1	8.6×10^{11}	63
Ramp	≈ 1	0.006	1.6×10^{13}	1200
Top energy	cont	1.0	0.8×10^{11}	97
	10	0.2	4.3×10^{11}	487

be minimized but cannot be avoided completely. Abnormal losses result from failure or irregular behavior of accelerator components. The design of the collimation system relies on the specified normal and abnormal operational conditions and if these conditions are met it is expected that the collimation system will work correctly and that components will not be damaged. It is assumed that the beams are dumped when the proton loss rates exceed the specified maximum rates.

Normal proton losses

Based on the experience with other accelerators it is expected that the beam lifetime during a fill of the LHC will sometimes drop substantially below the normal value. The collimation system should be able to handle increased particle losses, in order to avoid beam aborts and to allow correction of parameters and restoration of nominal conditions. In particular, the range of acceptable lifetime must allow commissioning of the machine and performance tuning in nominal running. For periods of up to 10 s beam lifetimes of 0.1 h (injection) and 0.2 h (top energy) must be accepted. The peak loss rate at injection energy occurs at the start of the ramp with an expected beam lifetime of 20 s for the first second of the ramp[1]. For continuous losses a minimum possible lifetime of 1 h is specified for injection and top energy. For details see [19]. Table 18.1 summarizes the specified lifetimes and the corresponding maximum power deposition in the cleaning insertion. The collimators should be able to withstand the specified beam load. At injection the protons impact on the material at a few micron from the collimator edge[20]. At 7 TeV this transverse impact parameter can be as small as a few hundred nanometer.

Low beam lifetimes can occur due to orbit and optics changes, e.g. during injection, start of ramp, or squeeze. Proton losses can therefore occur locally at a single collimator jaw, where they develop into nuclear showers. The lost energy is only to a small extent dissipated in the jaw itself; the downstream elements and the surrounding materials absorb most of the proton energy.

Abnormal proton losses

Much effort has been invested into a powerful LHC machine protection system, designed to handle equipment failures [21]. Primary proton losses will occur at the collimators if they are at nominal positions. The beam loss at the jaws is continuously monitored with fast Beam Loss Monitors [23, 24]. In case an abnormal increase of beam loss signal is detected, a beam abort is initiated and will be completed within 2-3 turns (178-267 μs). The beam is dumped before it can damage any accelerator components, including the collimators. The reliability of this process must be very high. For a detailed description see Chapters 15 and 17. Here it is assumed that in case of equipment failure the disturbed beam will always end up in the beam dump. However, this machine protection philosophy does not protect against single turn problems like irregularities of the beam dump itself and abnormally injected beam.

For these fast losses any jaw can be hit, because the primary collimators only cover one phase space location

[1] About 5% of the total intensity is expected to be uncaptured beam. It will be lost at the start of the ramp. The loss rate can be adjusted by the speed of the ramp.

Table 18.2: The beam deposited in the collimators for a few important one turn failures.

Abnormal condition	Beam energy [TeV]	Intensity deposit [protons]	Energy deposit [kJ]	Transverse dimensions [mm×mm]	Impact duration [ns]	Affected plane
Injection error	0.45	2.9×10^{13}	2073	1.0×1.0	6250	H/V/S
Asynchronous beam dump	0.45	6.8×10^{11}	49	$\boldsymbol{5.0} \times 1.0$	150	H
(all modules)	7.00	4.8×10^{11}	538	$\boldsymbol{1.0} \times 0.2$	100	H
Asynchronous beam dump	0.45	10.2×10^{11}	74	$\boldsymbol{5.0} \times 1.0$	225	H
(1 out of 15 modules)	7.00	9.1×10^{11}	1021	$\boldsymbol{1.0} \times 0.2$	200	H

and the overall LHC tune will vary. The collimator hardware must be designed to withstand the beam impact during abnormal proton losses without damage. The specified one turn beam loads on the collimator jaws are summarized in Table 18.2 for different abnormal conditions. The calculation assumes nominal bunch intensity (1.15×10^{11}), the nominal bunch scheme (2808 bunches separated by 25 ns), an average β_x of 410 m at the extraction kicker (MKD), and impact on the collimators between 5 and 10 σ_x. The energy deposition is integrated in time. The transverse dimensions listed in bold italic font are defined as full width (flat distribution) and all others are Gaussian standard deviations. Two cases of abnormal beam dump actions have been identified [16, 25]:

- The firing of the dump kickers is not synchronous with the beam dump gap, such that the LHC beam is swept across the aperture by the rising kicker voltage ("asynchronous dump").

- When one of the 15 MKD dump kicker modules spontaneously triggers it is followed by a re-trigger for the 14 other modules which will almost certainly be out of phase with the beam abort gap ("single module pre-fire"). The retriggering time is 1.2 μs at 450 GeV and 0.7 μs at 7 TeV [26].

The frequency of such failures is difficult to predict. It is assumed that they will happen at least once per year. A detailed discussion on the beam dump and its reliability is given in Chapter 17.

The impact of 7 TeV protons on a primary collimator for a single module pre-fire with the presently assumed MKD performance is shown in Fig. 18.1. It is assumed that protons between 5 σ_x and 10 σ_x can impact on a collimator (shaded area). Local dump protection devices are assumed to intercept all beam above 10 σ_x. This case is more severe than an asynchronous beam dump and the horizontal beam distribution on the collimator jaw is not flat. For a pre-fire of MKD 15 about 8 nominal LHC bunches impact over 5 σ_x (1 mm), close to the edge of the collimator. Note that abnormal dump actions only affect horizontal collimators, as the dump kick acts on the horizontal plane. To a lesser extent skew collimators can also be hit.

Injection oscillations can originate from the SPS extraction system, the pulsed transfer line magnets, or the LHC injection system (see Chapter 16). The transfer line collimation system (described in Volume 3 of the design report) will protect against several possible injection problems [27]. However, there are a number of residual cases which must be considered:

- The initial transfer line collimation system (two betatron collimators per plane) will ideally protect against injection oscillations at 7.5 σ amplitude, if these are generated upstream of the collimation system. Adding additional injection jitter from LHC injection (on the order of 0.5-1 σ) it is seen that primary and secondary collimators can be hit by a full injected batch. It is noted that the cold LHC aperture would be protected. An upgrade phase of the transfer line collimation system could constrain injection oscillations at the end of the transfer line to a maximum amplitude between 5 σ and 6 σ [28].

- Failures downstream of the transfer line collimation system cannot be protected against by this system (see also Chapter 15).

- A special flash-over failure has been identified for the LHC injection kicker. This failure can put 80% of an

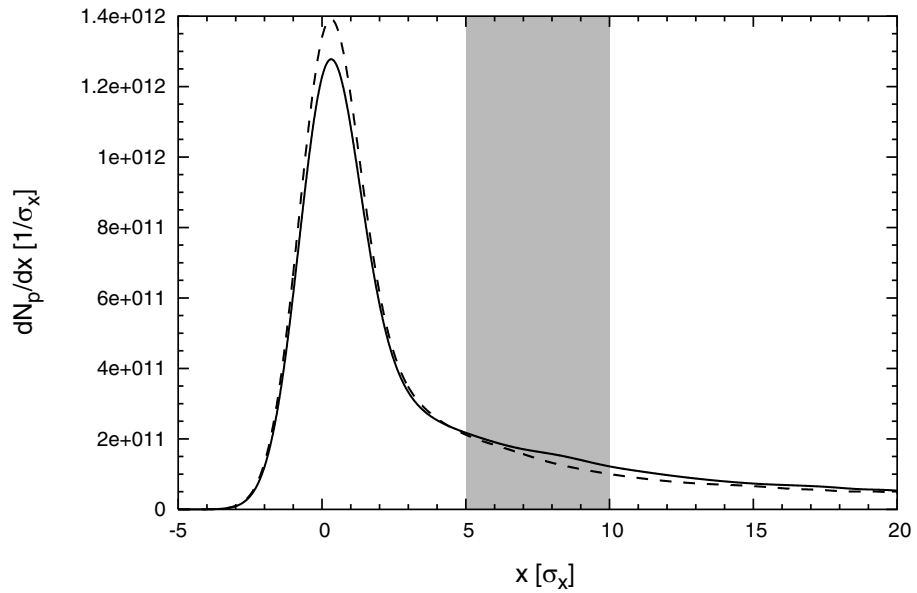

Figure 18.1: Time integrated horizontal distribution of LHC proton beam downstream of the MKD dump kickers, after a single module pre-fire. The two curves refer to a pre-trigger of the first and last kicker module, defining the two extreme cases. The shaded range shows the maximum collimator exposure.

injected batch onto a collimator jaw. Some further improvement would allow to reduce the beam impact to 50% of a batch. Expected frequency of a dangerous flash-over failure is about once per 10 years [29].

Based on this analysis of injection failures it is assumed that the amplitude of an oscillation can reach 6-10 σ and can affect both planes. The collimator jaws should therefore withstand the impact of a full injected batch without damage. It is noted that this design decision also decouples operation of the transfer line and ring collimation systems.

18.2.2 Definition of cleaning inefficiency

The following section contains a short introduction to the formal notation and central definitions for beam cleaning (see also Chapter 4). Halo particles are characterized by their normalized offsets $A_{x,y}$ in the transverse coordinates x, y:

$$A_x \;=\; \sqrt{\left(\frac{x}{\sqrt{\epsilon_x \beta_x}}\right)^2 + \left(\frac{\alpha_x x + \beta_x x'}{\sqrt{\epsilon_x \beta_x}}\right)^2}\,. \tag{18.1}$$

The same definition applies for A_y. Note that x is the sum of the betatron oscillation x_β and the dispersion offset δD_x, where D_x is the dispersion and δ the energy offset of the particle. Similar for x', y and y'. The terms β, α, and ϵ are the beta and alpha Twiss functions and the emittance. The normalized radial amplitude A_r of a particle is:

$$A_r = \sqrt{A_x^2 + A_y^2}\,. \tag{18.2}$$

The collimation system will capture most particles with large radial amplitudes. However, a secondary halo is generated from the primary collimators and a tertiary halo is leaked from the secondary collimators (see Fig. 18.2). In order to define the cleaning inefficiency η_c a variable normalized ring aperture a_c is considered. For N particles impacting at the collimators the cleaning inefficiency is then defined as the following leakage rate:

$$\eta_c(a_c, n_1, n_2) = \frac{1}{N}\sum_{i=1}^{N} H(A_r - a_c)\,. \tag{18.3}$$

Here, H is the Heaviside step function, returning 1 for $A_r \geq a_c$ and zero otherwise. The cleaning inefficiency gives the fraction of protons impacting on the primary collimators, which escape the collimators and reach at

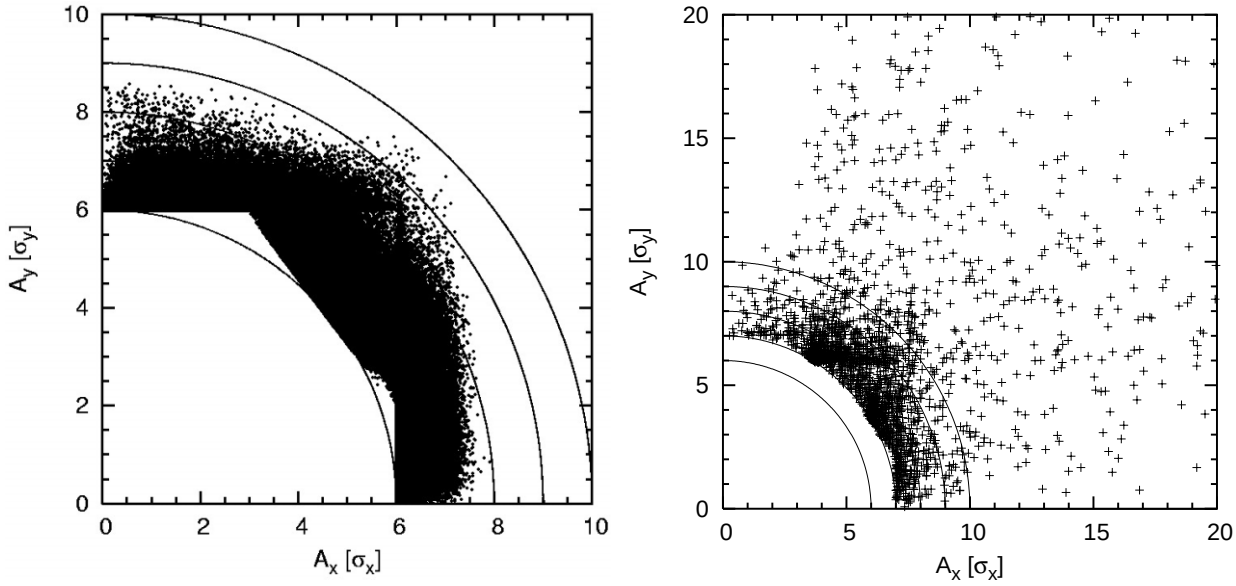

Figure 18.2: Transverse distribution of secondary (left) and tertiary (right) beam halos in normalized units. The primary and secondary collimators have been set to 6 σ and 7 σ in this example.

least a normalized ring amplitude a_c for given settings n_1 and n_2 of primary and secondary collimators. These protons will be lost into the cold aperture around the ring. Losses are diluted over some length L_{dil} and a local cleaning inefficiency $\tilde{\eta}_c = \eta_c / L_{dil}$ is defined. The cleaning inefficiency is determined with sophisticated tracking programs [30, 31, 32, 33] over many turns, counting each particle once[2].

18.2.3 Maximum leakage rates for protection against quenches

The maximum leakage rates or in other words the required cleaning inefficiency can be specified from the maximum loss rates, the quench limit, and the dilution length. The quench level R_q is estimated to be 7×10^8 protons/m/s for 450 GeV and for slow, continuous losses [2]. For 7 TeV a value of 7.6×10^6 protons/m/s is obtained (at top energy additional limits can arise for the heat load in an LHC sector). It is noted that transient losses over ≈10 turns must be controlled to about 10^{-9} of the total intensity for avoiding quenches. It was not possible to specify beam loss processes on this time scale and the required collimation inefficiency is therefore defined for slow, continuous losses. The longitudinal loss distribution is case dependent. For some specific case studies an average dilution length $L_{dil} = 50$ m is assumed. An accurate determination of L_{dil} remains to be completed. The total intensity N^q_{tot} at the quench limit R_q and for an operationally required minimum beam lifetime τ_{min} is then given by:

$$N^q_{\text{tot}} = \frac{\tau_{\text{min}} \cdot R_q}{\tilde{\eta}_c} \,. \tag{18.4}$$

The total intensity allowed at the quench limit is shown as a function of the local collimation inefficiency in Figure 18.3. It is assumed that a minimum beam lifetime of 0.2 h at top energy and 0.1 h at injection must be ensured for operation (see Table 18.1). It is noted that the most stringent requirements on the collimation inefficiency arise at top energy. The nominal intensity of 3×10^{14} protons per beam requires a collimation inefficiency of 2×10^{-5} m^{-1}. Injection has less strict requirements. The settings n_1, n_2 and n_3 of primary, secondary and tertiary collimators must be carefully adjusted in order to minimize the leakage rates of the cleaning insertions.

[2]This definition assumes that a particle that reaches a_c is lost within the same turn and cannot perform multiple revolutions.

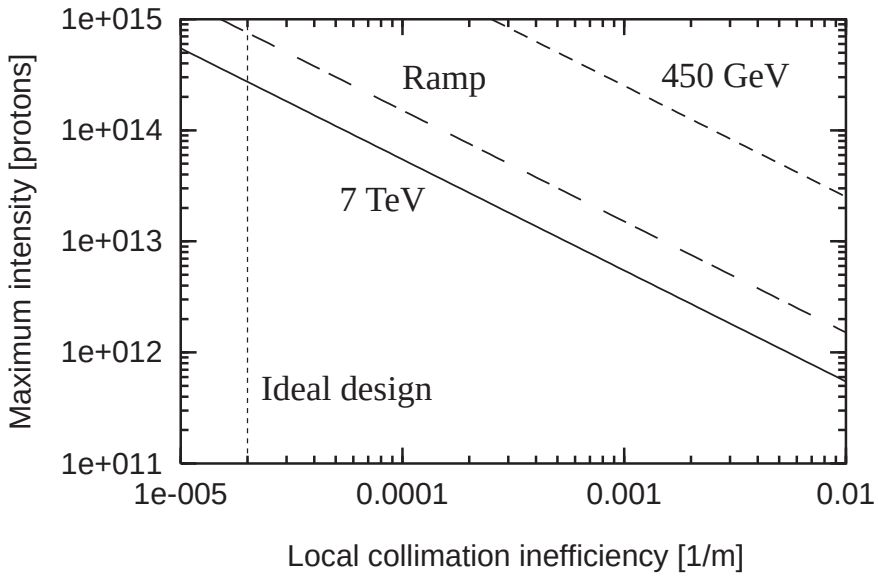

Figure 18.3: The maximum total intensity is shown as a function of the local collimation inefficiency for injection, top energy, and the start of the ramp. A beam lifetime of 0.2 h at top energy and 0.1 h at injection is assumed. The ideal design value for local inefficiency is indicated.

18.2.4 Constraints for collimator settings

The settings for the collimators are specified as the normalized half gap, assuming nominal emittance and the beta functions at the collimators. A setting n_1 of a primary vertical collimator means that the jaws are located at vertical positions of $\pm n_1 \cdot \sqrt{\epsilon_y^{\text{nom}} \cdot \beta_y^{\text{coll}}}$. This notation should not be taken as an indication that collimator settings depend on beam emittance; they must be decided based on the available machine aperture a_e. Several boundary conditions constrain the settings of the collimators. Nominal collimator settings for nominal intensity are 6 σ for primary and 7 σ for secondary collimators, both at injection and at 7 TeV with nominal β^*.

Machine protection functionality

The collimators in the warm insertions must be the aperture bottlenecks in the LHC ring. Therefore they cannot be opened to arbitrarily large gaps. For example, with the injection ring aperture designed for $n_1 = 7$ (aperture notation) the guaranteed minimal vertical aperture is 8.4 σ_y. Vertical protection devices like the TDI must then sit at around 7.5 σ_y and secondary vertical collimators should be set to around 7 σ_y. Betatron collimator settings at injection are constrained to be below 6 σ for primary and 7 σ for secondary collimators. The protection requirements at 7 TeV are a function of the values for β^* in the interaction points and the corresponding aperture bottleneck at the experimental triplets. The maximum allowed collimator gaps can be directly expressed as a function of the lowest β^* in the ring.

Quench prevention

The protection of the LHC aperture against loss of primary protons is not sufficient to prevent quenches of the super-conducting magnets. As seen in Figure 18.2 primary and secondary collimators generate a secondary and tertiary halo that extends several σ beyond the collimator settings. The collimators are conventionally put to a position such that the secondary halo does not impact on any super-conducting magnet.

Operational and accelerator physics constraints

It is beneficial for machine protection and halo cleaning to close the collimator gaps as far as possible. However, operational and accelerator physics constraints put important limitations on the allowed minimal collimator gap:

- The beam core must not be scraped by collimation, usually requiring collimator settings above 4-5 σ.
- The collimator gap must be wide enough to avoid excessive impedance from the collimators and to maintain beam stability. E.g. it may in most cases not be possible to reduce emittance and to move collimators to smaller gaps with the same normalized setting.
- The two-stage functionality of the collimation system must be maintained during the whole operational cycle, e.g. the primary collimators must always remain primary and the secondary must always remain secondary collimators. Usually a relative offset of 1 nominal $sigma$ is required, corresponding to about 200 μm at 7 TeV. Operational and mechanical tolerances are specified for this retraction. Maintaining the same normalized collimator gaps (e.g. 6 σ and 7 σ) with smaller than nominal emittances will be challenging.

Abort gap cleaning

Special considerations apply for the momentum collimators. Momentum collimation is needed to absorb a flash of losses soon after the beginning of the ramp [34, 35] and to capture off-bucket protons which loose momentum by synchrotron radiation at top energy [36, 37]. Long storage time of particles with large momentum offset must be avoided. Their detuning with momentum can be quite large (the momentum aperture of the ring is $\approx 6 \times 10^{-4}$) and thus the effective aperture may differ from the nominal one. In addition, these particles creep along the bunch structure and invade the abort gap. If their density is too large, a quench will occur in the magnets downstream the dump system even during normal beam dumps. The phenomenon is similar to the dump error discussed in Section 18.2.1. A detailed description of this effect is in preparation [38] and is illustrated in Figure 18.4. The peak density in the abort gap is given here by the very simplified expression

$$\hat{\rho}_0 \simeq 0.7 \, \frac{N_0}{\tau_{\rm long} L_{\rm ring}} \frac{\delta_{\rm cut}}{\dot{\delta}} = 2.2 \; 10^7 \;\; {\rm p/m} \, , \tag{18.5}$$

with N_0 the number of stored protons, $\tau_{\rm long} = 10$ h a somewhat low longitudinal beam lifetime, $L_{\rm ring} = 26660$ m, $\dot{\delta}_{cut} \simeq 10^{-3}$ the momentum cut made by the momentum collimation system at top energy and $\dot{\delta} = U_0 f_r / E_{\rm beam} = 10^{-5}$ the momentum loss per second by synchrotron radiation with $U_0 = 7$ keV/turn, $E_{\rm beam} = 7$ TeV and $f_r = 1.1 \times 10^4$ Hz the rotation frequency. The coefficient 0.7 is obtained by the integration of the synchrotron motion between $\delta_{\rm bucket}$ and $\dot{\delta}_{\rm cut}$ and by summing over all occupied buckets. This value is case specific and should only be used indicatively, see [38] for a complete formalism. The peak density is reached at the rear side of the abort gap, because particles with negative δ_p creep forward. In our case, the density at the head is $\rho_{\rm head} \approx \hat{\rho}_0/2 = 1.2 \times 10^7 {\rm p/m}$. This value is larger than the critical $\rho_{\rm tol} \approx 0.4 \times 10^7$ p/m, above which a quench is induced behind the dump system [39]. It is intended to make use of the transverse damper (see Chapter 6), used in an excitation mode, in order to increase the betatron amplitude of the particles which are present in the abort gap, and thus accelerate their capture. It is fortunate that the dangerous part of the abort gap is located at its head (this is where the dump kicker starts to rise and sprays the beam at low amplitude), because the creeping protons must traverse the entire gap before reaching the head. This allows the damper to work mostly in the central part of the gap, leaving enough time for turning the excitation mode on and off.

18.2.5 Layout goals

In order to achieve the required low inefficiencies of around 10^{-3} (before dividing by the dilution length) several design principles have been developed and included in the layout of the LHC collimation system:

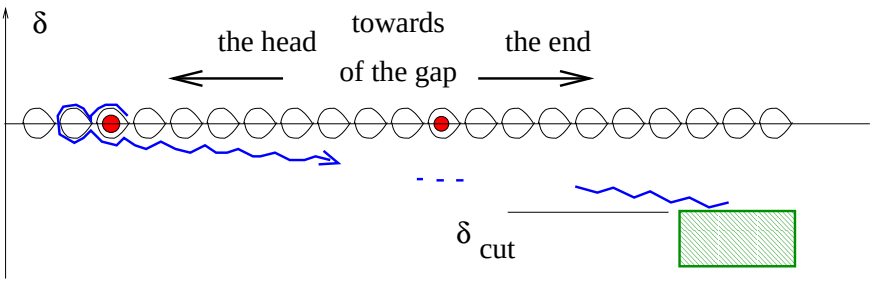

Figure 18.4: The longitudinal motion of a proton which left the bucket. It looses momentum by synchrotron radiation and is finally captured by the primary momentum collimator in IR3.

- A multi-stage cleaning process is implemented. Primary collimators intercept the lost primary protons and generate an on-momentum and off-momentum secondary proton halo. The secondary proton halo is intercepted by the secondary collimators which leak only a small tertiary halo. The tertiary halo is lost in the cold aperture but is populated sparsely enough that quenches are mostly avoided (see Figure 18.2). Tertiary collimators are used locally to provide additional protection from the tertiary halo (e.g. at the aperture bottlenecks in the triplets).

- The phase advances between different collimators and their orientations are optimized to achieve the best possible coverage in the x-x'-y-y' phase space [40, 41]. An additional optimization is performed to locate collimators at larger values of the beta function, thus obtaining larger opening gaps and a reduced impedance.

- As far as possible, collimators are located in front of bending magnets so that a large fraction of the proton-induced cascade is then swept out of the machine aperture and neutral particles do not propagate far downstream (see the dogleg description for IR3 and IR7 in Chapter 3).

- Separately optimized cleaning systems are dedicated to the cleaning of protons with high betatron amplitudes (betatron cleaning in IR7) and off-momentum protons (momentum cleaning in IR3). See the description of optics goals for IR3 and IR7 in Chapter 4.

- The collimators have been located in warm sections of the machine because the warm magnets are much more tolerant to local beam losses and can accept the particle showers that exit the collimators.

These constraints are implicitly included in the design of the LHC collimation system.

18.2.6 Radiological considerations

The cleaning insertions become some of the most activated sections at the LHC. For radiation studies it is estimated that about 30% of all stored LHC protons will be lost in the cleaning insertions at Points 3 and 7. Detailed radiological assessments were performed and are discussed in Volume 2 of this report. Of particular importance for maintenance are estimates of remanent dose rates from induced radioactivity. As studies have shown, these dose rates depend strongly on various factors, such as on the collimation layout, local shielding, the materials chosen, the cooling time and the location of the collimators within the beamline layout. Close to the collimators dose rates from activated beamline components or shielding typically reach several tens of mSv/h, whereas the dose rate from the collimator jaws (on close contact) can be significantly higher. The design of the collimators and adjacent equipment (high reliability, fast connections, ...) takes into account the fact that intervention time in these regions will have to be limited. It has been shown for the former layout (LHC layout and optics version 6.2) that the warm magnets and other accelerator equipment in the cleaning insertions can withstand the expected radiation [42]. However, the accumulated dose in the collimator tanks and the surrounding shielding is expected to be 1-100 MGy/year, thus rather radiation hard equipment will have to be installed. This significantly exceeds CERN's acceptable radiation dose to standard cables of 500 kGy as

given in [43]. Since the shielding layout will be different as assumed in preceding calculations [42], further detailed studies might become necessary.

18.2.7 Compatibility with the LHC ultra high vacuum

The choice of collimator design and materials must be compatible with the ultra-high vacuum of the LHC. The collimators must be bakeable and outgassing rates must remain acceptable.

18.2.8 Compatibility with the LHC impedance budget

The collimators can produce significant transverse resistive impedance due to the small gaps at 7 TeV (impedance scales inversely proportional to the third power of gap size). Some increase of the LHC impedance can be handled with the LHC octupoles, which provide Landau damping of the rigid dipole modes. The collimator-induced impedance, the impedance limit, and the beam stability with collimators are discussed in detail in Chapter 5. The compatibility of the collimation system with the LHC impedance budget is a limiting design constraint for the collimators.

18.3 THE CONCEPT OF A PHASED APPROACH FOR LHC COLLIMATION

A detailed analysis of possible collimator materials and concepts did not produce any single collimator solution that fulfills all the design goals for LHC collimation (see also discussion in section 18.5). In particular it was found that a trade-off exists between collimator robustness and collimator induced impedance. For example, a collimation system with sufficient robustness (based on graphite material) would introduce peak performance limitations for the LHC (reduced intensity, increased β^*). A system with sufficiently low impedance (copper based) would likely experience regular damage to the collimator jaws with resulting loss in cleaning inefficiency (peak intensity) and efficiency of LHC operation. A beryllium based system would not resist the specified one turn beam loads and in addition would introduce concerns about toxic materials.

In order to in spite of these problems meet the LHC design goals, a number of sub-systems have been defined which have specific tasks and which can conveniently be fitted into different installation phases. The system for beam cleaning and collimation in the LHC will be constructed and installed in three phases [44]. This phased approach relies on the fact that difficulties and performance goals for the LHC are distributed in time, following the natural evolution of the LHC performance. The phased approach allows initial operation with a collimation system with fewer components than previously foreseen. The following section describes the different phases and the associated philosophy of beam cleaning and collimation.

18.3.1 Phase 1

The initial phase 1 system will be the central part of the overall collimation system. It will be described in more detail later. Essentially this phase presents a collimation system with maximum robustness which includes a reduced two-stage cleaning in IR3 and IR7, tertiary collimators at the experimental insertions, scrapers, and special collimators for injection protection in IR2/IR8 and collision debris in IR1/IR5. The phase 1 collimation system is designed to withstand the specified beam impact and will be the system to be used for injection and ramp up to nominal or even ultimate intensities. The normalized settings of main collimators and the predicted cleaning inefficiency are listed in Table 18.4. The injection set-up with phase 1 collimation is illustrated in Fig. 18.5. A two-stage cleaning process is performed with primary and secondary collimators at 6 σ and 7 σ (here referring to σ at injection). The cold aperture limitation in the LHC arcs is efficiently shadowed. This set-up is used during the whole lifespan of the LHC. Scrapers can be used for beam forming or halo diagnostics.

During collisions at 7 TeV, the phase 1 collimation system may be operating at the impedance limit, limiting the maximum intensity and thus LHC luminosity. The three-stage 7 TeV set-up during phase 1 collimation is illustrated in Fig. 18.6. The C collimators in IR7 are set for relaxed conditions with half intensity and $\beta^* = 1$ m. A three-stage cleaning process is then performed with primary and secondary collimators at 6 σ and 8.5 σ (here

referring to σ at 7 TeV). Tertiary collimators in the experimental insertions provide additional shadow for the super-conducting triplet magnets.

The technical design of the collimators in phase 1 is demanding but follows conventional concepts. Mechanical and operational tolerances at 7 TeV can be relaxed by a factor larger than 3 with respect to the full performance system, if a higher β^* is accepted.

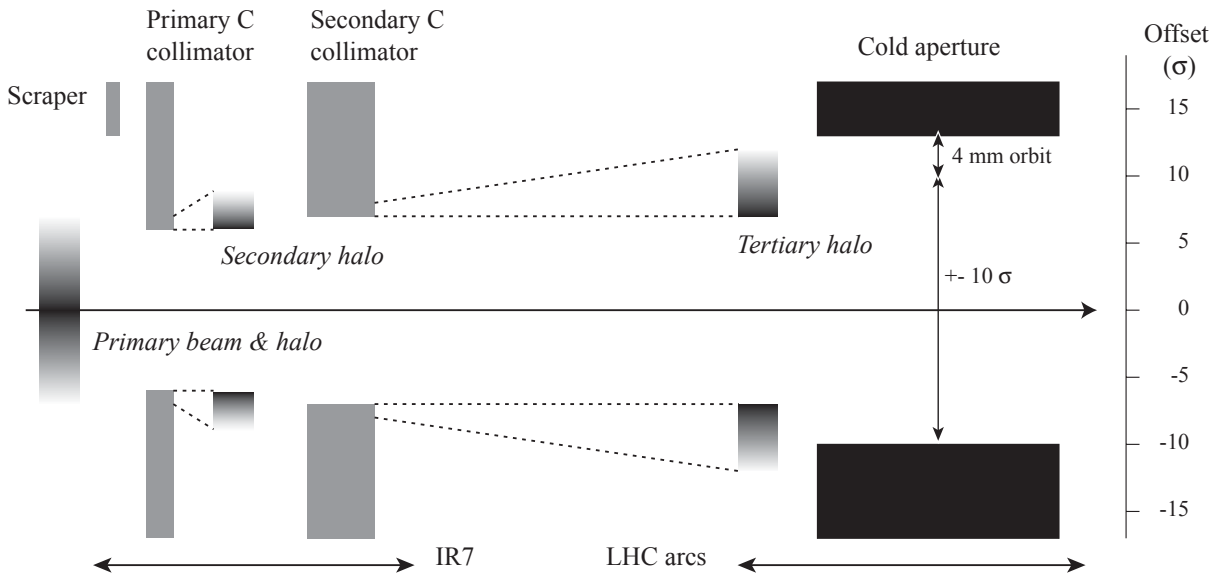

Figure 18.5: Principle of betatron collimation and beam cleaning at *injection energies* and during the ramp.

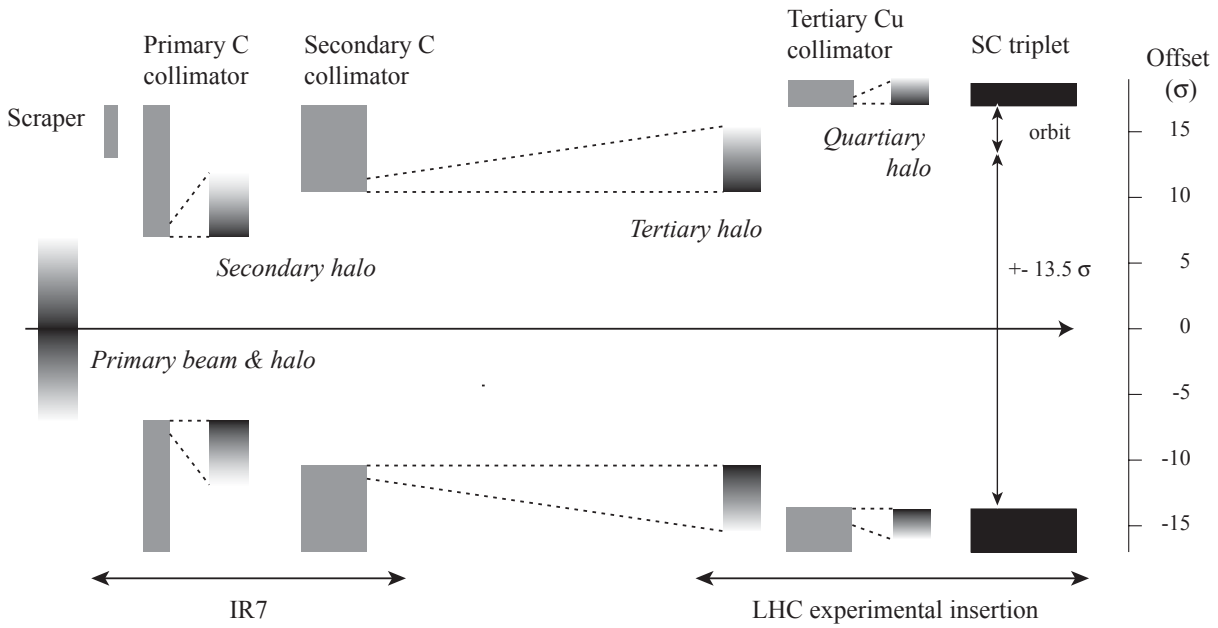

Figure 18.6: Principle of betatron collimation and beam cleaning *during collisions* in phase 1. The C collimators in IR7 are set for half intensity and $\beta^* = 1$ m.

18.3.2 Phase 2

The phase 2 system will complement the high robustness secondary collimators in IR3 and IR7 with 30 low impedance "hybrid" collimators. These hybrid collimators, which will only be used towards the end of the low beta squeeze at 7 TeV and in stable physics, will have a reduced robustness but low impedance and excellent

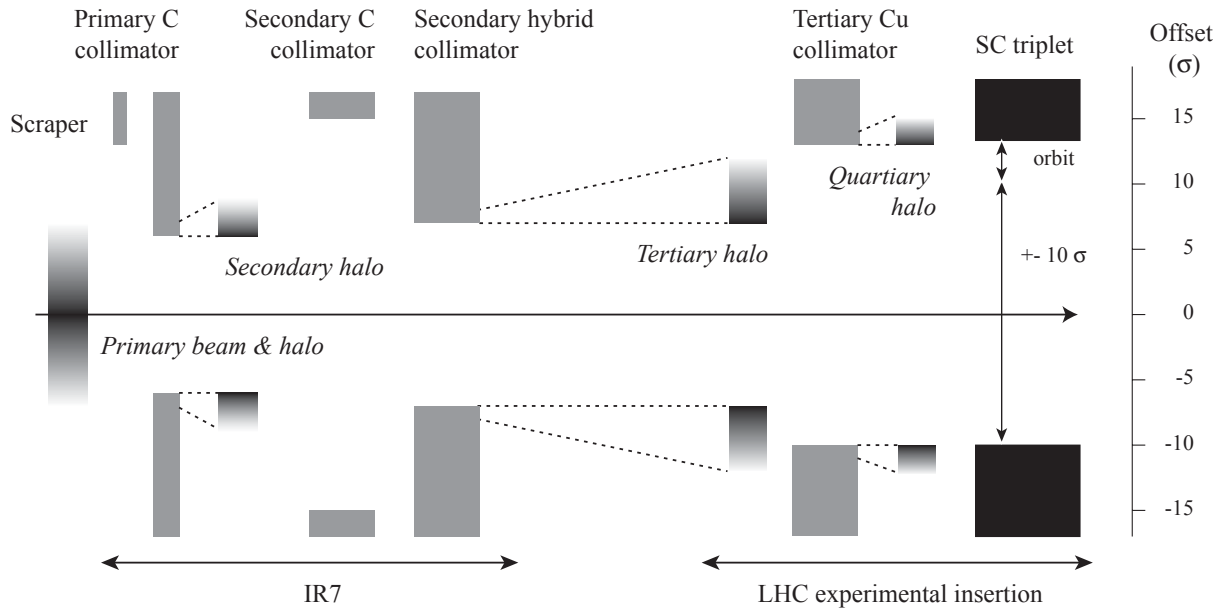

Figure 18.7: Principle of betatron collimation and beam cleaning during *collisions in phase 2*. Hybrid secondary collimators with low impedance are used, allowing nominal intensity and β^* with nominal collimation gaps.

mechanical tolerances and will support nominal performance. The 7 TeV set-up for phase 2 collimation is illustrated in Fig. 18.7. Hybrid secondary collimators with low impedance are used, allowing nominal intensity and β^* with nominal collimation gaps. A three-stage cleaning process is performed with primary and secondary collimators at 6 σ and 7 σ (here referring to σ at 7 TeV). Tertiary collimators in the experimental insertions provide additional shadow for the super-conducting triplet magnets. Scrapers can be used for beam forming or halo diagnostics.

The hybrid collimators will only be used in stable conditions at top energy, when risk of damage is significantly reduced. Only a few horizontal collimators can be affected by abnormal beam loss because several scenarios for abnormal beam impact do not apply at 7 TeV. Either the design of the collimators will be able to cope with possible damage ("consumable" collimator concept) or the critical collimators[3] can be retracted into the protection of the local dump absorber TCDQ (see Chapter 17), accepting reduced cleaning efficiency and higher normal losses on the TCDQ.

The design of the hybrid collimators is not decided yet. The possible options include consumable metallic collimators, a graphite material doped with copper, beryllium jaws, thick metallic coating and graphite jaws with a movable metallic foil. For performance estimates we assume a consumable collimator design with a 1 m long Cu jaw.

18.3.3 Phase 3

Several years after LHC start-up, 4 additional collimators will be installed in order to capture the high luminosity collision debris downstream of IR1 and IR5. These devices will be required once LHC exceeds about 30% of the nominal design luminosity.

18.3.4 Phase 4: Eventual efficiency upgrade

The collimation sub-systems in IR3 and IR7 were reduced by 16 collimators in order to reduce the number of components (total cost, work load for phase 1) and to limit their contribution to impedance. Compared to the full complement of collimators, the associated cost in performance is a factor 2 loss in efficiency. Placeholders are kept for all suppressed collimators. If LHC operation reveals problems with cleaning efficiency, the best

[3]For a known tune working point it can be predicted accurately which horizontal collimator is exposed to abnormal dumps.

Table 18.3: Overview on the different types of collimators used in the LHC ring collimation system for both beams and for phases 1-3. The jaw length is given without impedance tapering.

Acronym	Material	Length [m]	Number	Locations	Purpose
TCP	C or C-C	0.2	8	IR3, IR7	Primary collimators
TCSG	C or C-C	1.0	30	IR3, IR7	Secondary collimators
TCSM	tbd	1.0	30	IR3, IR7	Hybrid secondary collimators
TCT	Cu	1.0	16	IR1, IR2, IR5, IR8	Tertiary collimators
TCLI	tbd	tbd	4	IR2, IR8	Injection protection
TCLP	Cu	1.0	8	IR1, IR5	Protection luminosity debris
TCSP	tbd	tbd	6	IR3, IR7	Beam scraping

possible cleaning efficiency and protection can be achieved by adding the 16 collimators.

18.4 THE IMPLEMENTATION OF THE PHASED APPROACH

The choice of a phased approach requires significantly more space for collimators than previously foreseen. For each secondary collimator a space of 4 m must be reserved for phase 1 and phase 2 collimators, almost 6 times more than in the former layout. Fewer collimators will be installed initially while a higher number of components is required for all four phases. A careful optimization was performed to optimize the cleaning insertions accordingly while maintaining cleaning efficiency and minimizing impedance. The phased solution is described in detail in this section.

18.4.1 Number of components, performance and schedule

A list of the collimator types, their material choice and length, number of components, locations, and purposes is given in Table 18.3. The number of components in the different phases, the main collimation settings for betatron and momentum cleaning, and predicted inefficiencies are listed in Table 18.4. The calculated inefficiency refers to the range of predicted values [45]. It does not include the cleaning from the tertiary collimators nor any imperfections in collimator settings. About 6 scrapers and a number of absorbers will additionally be installed for phase 1. An optional phase 4 would provide for a modest upgrade in cleaning inefficiency and would only be pursued in the case of unforeseen problems. It is noted that inefficiencies at injection seem adequate, while the situation at top energy cannot be guaranteed to be adequate and therefore the tertiary collimators have been introduced. The phase 1 installation will be available for the LHC start-up and commissioning. Phase 2 collimators will be installed 1-2 years and phase 3 collimators about 3 years after the first physics runs.

18.4.2 IR7 layout

The IR7 insertion contains the betatron collimation system. Optics and aperture properties of the IR7 layout are described in Chapters 3 and 4. An efficient design process for IR7 took into account the space requirements, all proposed collimators, impedance minimization and efficiency optimization. During this process collimators were moved up to 30 m and quadrupoles up to 1 m. Additional design optimizations for vacuum layout and beam instrumentation were included. The finally adopted longitudinal layout is summarized in Figure 18.8, clearly indicating phase 1 and phase 2 secondary collimators, as well as placeholders for further upgrades.

18.4.3 IR3 layout

The IR3 insertion houses the momentum collimation system. Much fewer components are used than in IR7 and a more limited redesign was performed in order to allocate the required spaces. Optics and aperture properties of the IR3 layout are described in Chapters 3 and 4. The finally adopted longitudinal layout is summarized

Table 18.4: Overview on the foreseen phases of LHC collimation. The total number of collimators N_{coll}, the settings n_1, n_2, n_3 and the expected ideal cleaning inefficiencies are listed for the different phases and machine states, and for betatron (IR7) and momentum (IR3) cleaning systems.

Phase	N_{coll}	Setting	Stages	n_1 [σ_β]	n_2 [σ_β]	n_3 [σ_β]	Performance	Cleaning inefficiency (ideal)
1	62	Injection IR3	2	8.0	9.3		Initial	
		Injection IR7	2	6.0	7.0			$(6.3\ldots12.6)\times10^{-3}$ at 10 σ_r
		Collision IR3	2	15.0	18.0			
		Collision IR7	3	6.0	8.5	14.0		$(0.5\ldots1.5)\times10^{-3}$ at 14 σ_r
		(β^*=1 m)						
		Collision IR7	3	6.0	7.0	10.0		$(1.1\ldots3.3)\times10^{-3}$ at 10 σ_r
		(β^*=0.5 m)						
2	92	Injection IR3	2	8.0	9.3		Nominal	
		Injection IR7	2	6.0	7.0			$(6.3\ldots12.6)\times10^{-3}$ at 10 σ_r
		Collision IR3	2	15.0	18.0			
		Collision IR7	3	6.0	7.0	10.0		$(0.2\ldots2.0)\times10^{-3}$ at 10 σ_r
3	96	Injection IR3	2	8.0	9.3		High lumi.	
		Injection IR7	2	6.0	7.0			$(6.3\ldots12.6)\times10^{-3}$ at 10 σ_r
		Collision IR3	2	15.0	18.0			
		Collision IR7	3	6	7	10.0		$(0.2\ldots2.0)\times10^{-3}$ at 10 σ_r
(4)	112	Injection IR3	2	8.0	9.3		Maximum	
		Injection IR7	2	6.0	7.0			$(5.7\ldots11.4)\times10^{-3}$ at 10 σ_r
		Collision IR3	2	8.0	9.3			
		Collision IR7	3	6.0	7.0	10.0		$(0.2\ldots2.0)\times10^{-3}$ at 10 σ_r

in Figure 18.9, including phase 1 and phase 2 secondary collimators. It is noted that no placeholders for future efficiency upgrades are required in IR3.

18.4.4 Radiological aspects of phased installation

The collimators will intercept a large fraction of the protons that are lost in the machine during normal operation. The induced showers activate the collimators themselves and the downstream equipment in IR3 and IR7. It is therefore essential to carefully study the radiological consequences and to consider provisions for minimizing the environmental impact and personnel exposure. Further details are given in Volume 2 of this report. The possibility of installation work and maintenance close to the collimators is an important aspect for the feasibility of the phased installation. Simulation studies have shown that residual activation can be significant, imposing strict limitations on any human intervention [46]. It is legally required to perform a detailed planning of each intervention with regard to personal and collective doses. An example study of the dose received during the exchange of a collimator showed that the personal dose may reach several tens of mSv [47, 48]. These results strongly depend on the particle losses at that collimator, the collimator material and the surrounding local shielding. As for dose planning more detailed calculations will have to be performed in order to understand and optimize the final layout of the collimators and its implication on collective doses (for example see [49]). During the first two years of LHC operation losses will be smaller and thus dose rates lower by about a factor of two. However, precautions have to be taken for the phase 2 installations in order to keep personal and collective doses as low as reasonably achievable (ALARA). Therefore, a fast installation procedure is foreseen and prepared from the design phase onward.

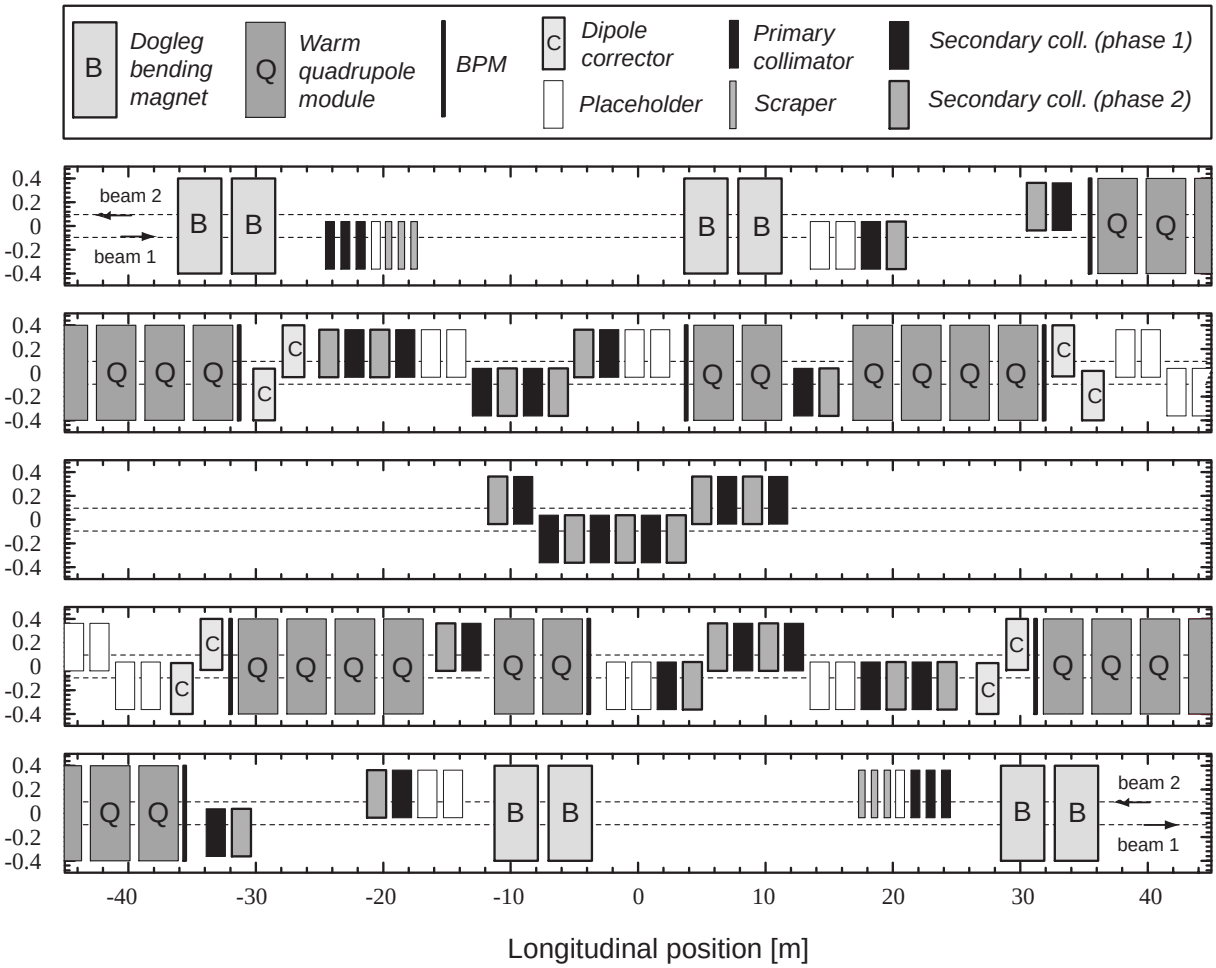

Figure 18.8: Longitudinal layout for the betatron cleaning insertion in IR7.

Table 18.5: Overview on the collimators installed for phase 1 of LHC collimation. The numbers refer to the total number of elements as required for both beams. Note that 6 scrapers have been included into this list. This is a sub-set of Table 18.3.

Acronym	Number	Locations	Purpose
TCP	8	IR3, IR7	Primary collimators
TCSG	30	IR3, IR7	Secondary collimators
TCT	16	IR1, IR2, IR5, IR8	Tertiary collimators
TCLI	4	IR2, IR8	Injection protection
TCLP	4	IR1, IR5	Protection luminosity debris
TCSP	6	IR3, IR7	Beam scraping

18.5 DESCRIPTION OF PHASE 1 COLLIMATION

Phase 1 of collimation will provide a collimation system with maximum robustness. It is accepted to operate at the LHC impedance limit and to reduce the luminosity reach somewhat below nominal performance. The system must be ready for the start-up of the LHC and will support commissioning and initial luminosity running without a further upgrade. For phase 1 it is foreseen to install 62 collimators and 6 scrapers. The numbers and types of components are given in Table 18.5. The collimation settings and expected performance have been summarized in the previous section. In this section a detailed list of phase 1 components is given, the basic hardware choices are explained and the mechanical design is presented.

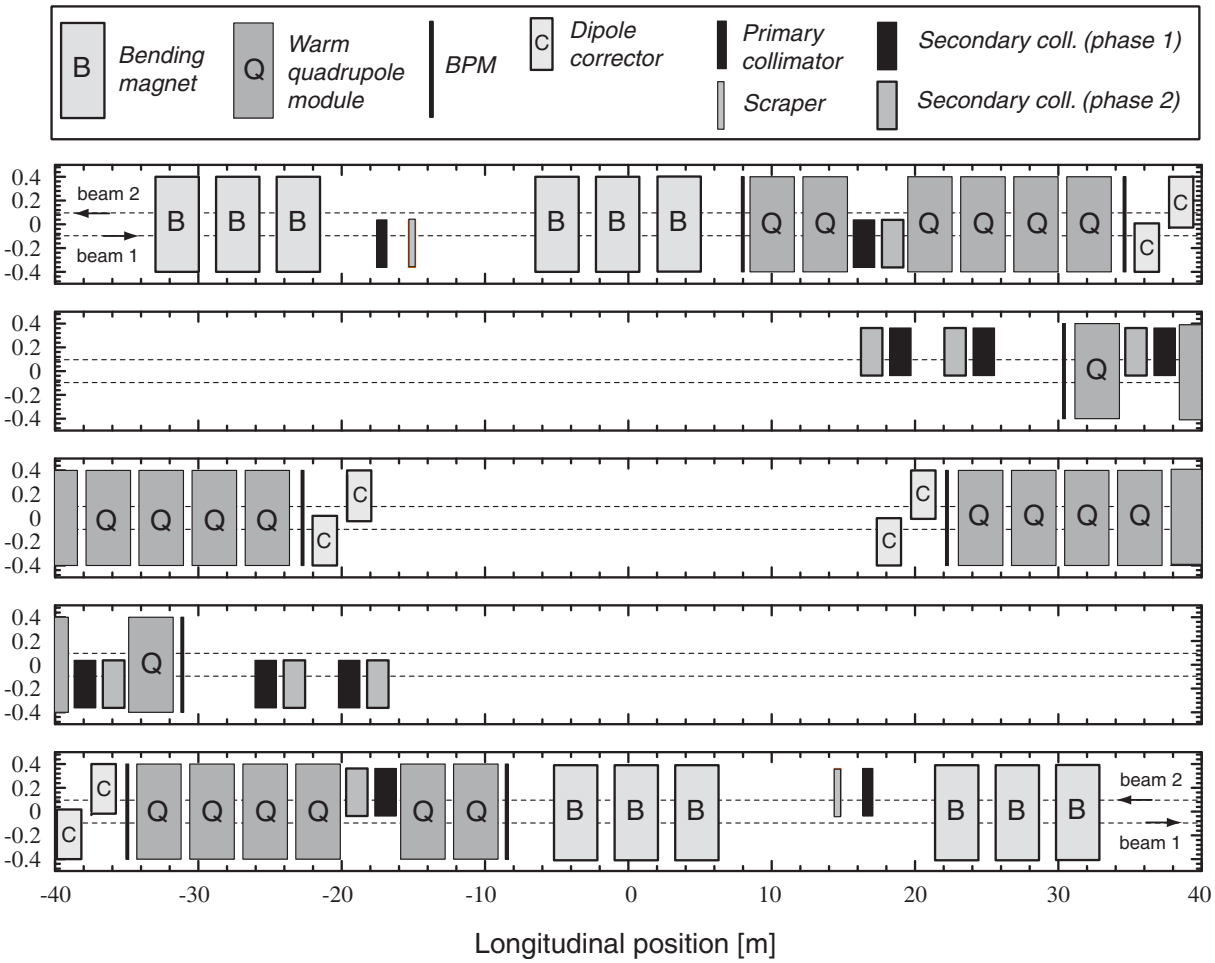

Figure 18.9: Longitudinal layout for the monetum cleaning insertion in IR3.

18.5.1 Components in IR3 and IR7

Detailed lists of phase 1 collimators are given in Tables 18.6 and 18.7 for the IR3 and IR7 collimation systems. The list specifies in particular the longitudinal position, the nominal half gap and the azimuthal orientation of the jaws. The nominal half gaps in the betatron cleaning refer to settings of 6 σ and 7 σ for primary and secondary collimators, a beam energy of 7 TeV, the design optics and the nominal 7 TeV emittance. Nominal 7 TeV settings in the momentum cleaning are 15 σ and 18 σ for primary and secondary collimators (expressed in betatron beam size). It is noted that the specified 7 TeV half gaps in both insertions are operationally challenging and cannot be reduced much further without significant effort.

18.5.2 High robustness graphite collimators for phase 1 (TCP/TCSG)

Collimators with maximum robustness are required for the phase 1 system. The decision was that a graphite material should be used for the LHC collimators [50] based on the specified maximum beam load on the collimators (see Section 18.2.1). Both fine grain graphite (carbon, C) and fiber-reinforced graphite (carbon-carbon, C-C) have sufficient robustness to withstand all specified beam load cases at injection and top energy without damage. Graphite materials exhibit a significant variation in electrical resistivity, ranging from 7 $\mu\Omega$m to about 30 $\mu\Omega$m. For impedance calculations an electrical resistivity of 14 $\mu\Omega$m (fine-grain graphite) was assumed [51]. The specific variety of graphite will be selected based on measurements to be made at CERN of electrical properties, vacuum performance, and mechanical tolerances.

Table 18.6: Collimators in the momentum cleaning insertion IR3 for beam 1 and beam 2. For each collimator the longitudinal position relative to IP3, the azimuthal orientation of the jaws and the nominal half gap at 7 TeV is listed. The list includes only phase 1 collimators; hybrid TCSM collimators are omitted.

Name	Distance from IP3 [m]	Azimuth [°]	Half gap [mm]
TCP.6L3.B1	-177.35	0	3.87
TCSG.5L3.B1	-142.31	0	2.94
TCSG.A4R3.B1	43.34	0	2.06
TCSG.A5R3.B1	55.20	170.4	2.72
TCSG.B5R3.B1	61.02	11.4	3.05
TCP.6R3.B2	177.45	0	3.64
TCSG.5R3.B2	143.31	0	2.63
TCSG.A4L3.B2	-42.34	0	2.14
TCSG.A5L3.B2	-54.20	170.9	2.60
TCSG.B5L3.B2	-60.02	10.5	2.84

Peak temperature increase

The energy deposition in Graphite and other materials due to a single module dump pre-fire at 7 TeV (compare Section 18.2.1) was calculated with FLUKA [52, 53]. The results are summarized in Table 18.8. It can be seen that graphite and beryllium exhibit a reasonable maximum temperature increase after impact of the 8 out of 2808 LHC bunches. Aluminium, titanium and copper show destructive maximum heating. The heating along the length of a collimator jaw is illustrated in Figure 18.10. The development of the particle cascade and the longitudinal position with maximum heating are visible. For a graphite secondary jaw (1 m length) the peak temperature is reached at the end of the jaw. Energy deposition was calculated for all specified beam load cases and for both protons and ions. The results indicated that graphite jaws meet the requirements of maximum robustness. They must have a transverse depth of at least 15 mm to avoid excessive showering in a higher-Z back plate.

Peak mechanical stress

The results of the FLUKA calculations were input to thermo-mechanical calculations, performed with ANSYS [50]. Table 18.9 summarizes the calculated peak stress values for load cases at injection and top energy and graphite, carbon-carbon (CFC), and beryllium materials. To compare the structural behavior of the jaw materials, a stress norm $\sigma_{equiv} = ||s||$ is introduced[54]. For beryllium this is a von Mises stress. The isotropic, fine grain graphite is estimated by the Stassi criterion (generalized von Mises). CFC is analyzed with its principal components in each direction. Corresponding to the main fiber orientation in the y-direction, the main calculated values are indicated in Table 18.9. The peak stresses are compared to the maximum allowed, which is specific for each material. Calculated peak stress values for graphite and carbon-carbon (fiber-reinforced graphite) are within the tolerances and can be used for maximum robustness collimator jaws, both for primary and secondary collimators. Beryllium does not meet the tolerances for either injection or 7 TeV load cases and cannot be used safely.

Heat load and cooling

During normal operation the collimators will experience a varying heat load from electro-magnetic fields (RF heating) and from direct beam deposition and an appropriate cooling system is required. The maximum heat load occurs at 7 TeV where up to 4×10^{11} p/s can be lost for 10 s (case of 0.2 h beam lifetime). The lost protons have impact parameters of 0-200 nm and a typical round spot size of 200 μm is assumed. This case was studied using the scattering routines in FLUKA [52, 53]. The energy is deposited in multi-turn interactions. It was found that the longitudinal power density depends on the beam-to-jaw collinearity. Small misalignments

Table 18.7: Collimators in the betatron cleaning insertion IR7 for beam 1 and beam 2 during phase 1. Placeholders for an eventual efficiency upgrade are included is slanted face (not installed during phase 1) and phase 2 TCSM collimators are omitted. For each collimator the longitudinal position relative to IP7, the azimuthal orientation of the jaws and the nominal half gap at 7 TeV is listed.

Name	Distance from IP7 [m]	Azimuth [°]	Half gap [mm]
TCP.D6L7.B1	-204.17	90.0	1.2
TCP.C6L7.B1	-203.17	0.0	1.7
TCP.B6L7.B1	-202.17	135.0	1.4
TCP.A6L7.B1	-201.17	45.0	1.4
TCSG.B6L7.B1	-165.67	41.1	1.7
TCSG.A6L7.B1	-161.67	141.5	1.7
TCSG.B5L7.B1	-102.27	146.7	2.0
TCSG.A5L7.B1	-98.27	40.5	2.0
TCSG.E4L7.B1	-76.97	90.0	1.3
TCSG.C4L7.B1	-47.77	134.4	2.1
TCSG.B4L7.B1	-6.97	0.0	1.9
TCSG.A4L7.B1	-2.97	135.7	1.8
TCSG.A4R7.B1	1.03	44.2	1.8
TCSG.B4R7.B1	49.73	135.7	2.1
TCSG.A5R7.B1	88.23	44.7	2.2
TCSG.B5R7.B1	92.23	134.0	2.2
TCSG.C5R7.B1	104.23	90.0	2.1
TCSG.D5R7.B1	108.23	57.9	2.1
TCSG.E5R7.B1	112.23	122.8	2.0
TCSG.6R7.B1	146.83	0.5	2.9
TCP.D6R7.B2	204.18	90.0	1.2
TCP.C6R7.B2	203.18	0.0	1.6
TCP.B6R7.B2	202.18	135.0	1.4
TCP.A6R7.B2	201.18	45.0	1.4
TCSG.B6R7.B2	165.48	41.7	1.7
TCSG.A6R7.B2	161.48	140.8	1.7
TCSG.B5R7.B2	102.26	146.6	2.0
TCSG.A5R7.B2	98.26	40.3	2.0
TCSG.E4R7.B2	76.93	90.0	1.3
TCSG.C4R7.B2	47.74	135.6	2.1
TCSG.B4R7.B2	11.00	0.0	1.9
TCSG.A4R7.B2	7.00	136.6	1.8
TCSG.A4L7.B2	-9.00	43.4	1.8
TCSG.B4L7.B2	-49.74	136.1	2.1
TCSG.A5L7.B2	-88.26	45.0	2.2
TCSG.B5L7.B2	-92.26	133.7	2.2
TCSG.C5L7.B2	-104.26	90.0	2.1
TCSG.D5L7.B2	-108.26	58.3	2.1
TCSG.E5L7.B2	-112.26	122.3	2.0
TCSG.6L7.B2	-146.72	0.5	2.9

Table 18.8: Density, maximum energy deposition, maximum temperature, and fraction of energy escaping a 1.4 m long collimator jaw of different materials for a single module dump pre-trigger at 7 TeV. Some materials are heated well above their melting point and it is noted that the temperature is given for illustration only.

Material	Density [g/cm^{-3}]	Max. energy deposition [GeV/cm^{-3}]	Max. temperature [°K]	Energy escaping [%]
Graphite	1.77	1.3×10^{13}	800	96.4
Beryllium	1.85	0.9×10^{13}	310	97.0
Aluminium	2.70	5.3×10^{13}	2700	88.8
Titanium	4.54	1.7×10^{14}	>5000	79.5
Copper coating (100μm)	8.96	7.0×10^{14}	>5000	34.4

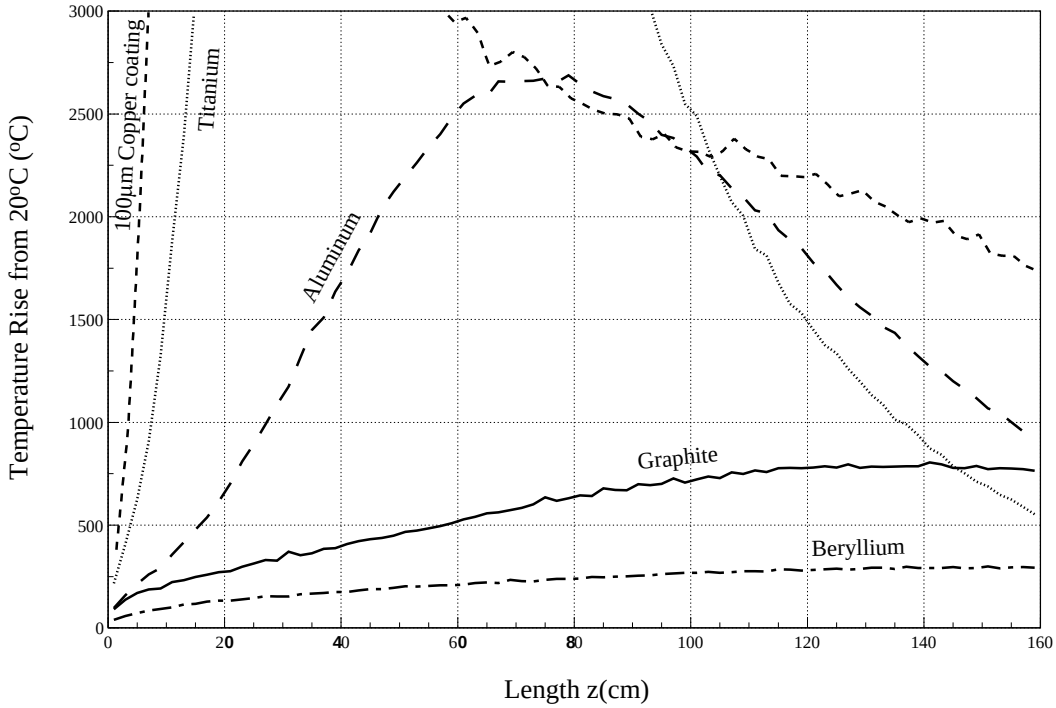

Figure 18.10: Maximum temperature increase for different longitudinal slices of a collimator block and for different materials. A single module dump pre-trigger at 7 TeV is assumed for a typical spot size of 200 μm.

reduce the length of traversal and energy is deposited in a shorter distance, e. g. a 5 μrad misalignment reduces the traversal length to 2 cm. This is illustrated in Figure 18.11. The proton induced power is then 2960 W which must be compared to a 1785 W for perfect alignment. The maximum possible peak power deposition from primary proton is expected to be close to 3 kW.

RF heating was estimated to be below about 0.5 kW per jaw. In addition comes the power deposition due to showers that originate in upstream collimators. Energy deposition in a secondary collimator was found to be up to 30 kW in phase 1 and 130 kW in phase 2. The maximum power deposition in a phase 1 collimator amounts to 34 kW for peak losses during 10 s. The maximum continuous power load for a specified beam lifetime of 1 h amounts to about 7 kW.

In conclusion, a secondary collimator with two jaws must withstand a power load of 34 kW during 10 s and 7 kW continuously in phase 1. An appropriate cooling system is under study with the goal to hold the jaw temperature below 50 °C and to prevent significant mechanical deformations.

Dedicated cooling systems are required for the two cleaning insertions. The systems will provide independent control of cooling water for each collimator. It is particularly important that the activated water can be drained and refurbished remotely during a collimator bake-out or a collimator exchange.

Table 18.9: Summary of calculated peak stress values σ_{equiv} for *impact of one injected batch* and for *7 TeV impact* of 8 out of 3000 bunches (abnormal dump) on a collimator. Different materials and primary and secondary collimator lengths are compared. The allowable maximum stress σ_{allow} is listed and the suitability is indicated.

Case	Material	Jaw length [cm]	Max. temperature [°C]	Stress σ_{equiv} [MPa]	σ_{allow} [MPa]	Suitability
Injection	Carbon-Carbon	20	335	4.4	86	yes
		100	345	12.7	86	yes
	Graphite	20	335	3.1	18	yes
		100	345	6.2	18	yes
	Beryllium	20	168	334	160	no
		100	200	440	160	no
7 TeV	Carbon-Carbon	20	212	20.8	86	yes
		100	551	82.0	86	yes
	Graphite	20	212	4.4	18	yes
		100	551	17.8	18	yes
	Beryllium	20	116	584	160	no
		100	168	1248	160	no

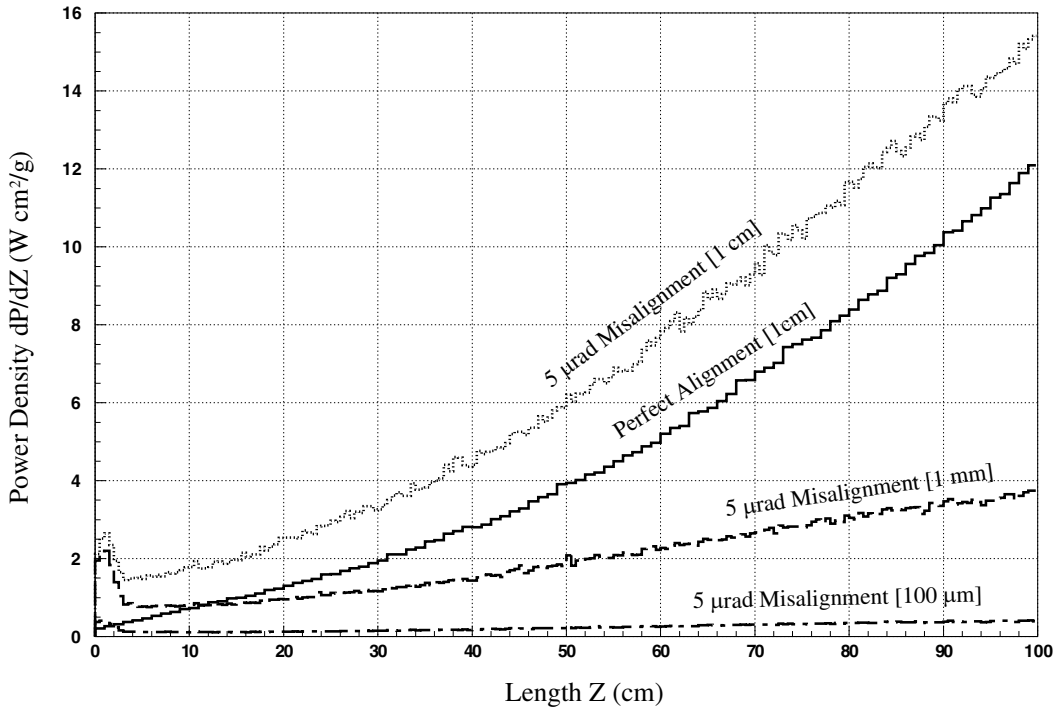

Figure 18.11: Longitudinal power density along a 1 m long graphite collimator, plotted versus the longitudinal position. It is assumed that 4×10^{11} p/s impact at 7 TeV with impact parameters of 0-200 nm (case of 0.2 h beam lifetime). The curves correspond to a perfect parallelism between protons and jaw (perfect alignment) and a 5 μrad misalignment. The power density is integrated in several transverse ranges of 0.1 mm to 10 mm.

Vacuum compatibility

The LHC beam tube is an ultra-high vacuum system and the collimators must not disturb vacuum performance. Several species of graphite were tested for outgassing rates and compatibility with the LHC vacuum requirements [55]:

- Variations in outgassing rate of up to a factor of 10 were observed for the materials tested. Material composition, dimensions and design are essential and each material/design must be examined separately.

- A factor of 10 improvement in outgassing rate can be achieved by heat treatment in a clean vacuum or a high temperature bake-out.
- An in-situ bake-out at above 300°C improves the performance by a factor of 10.
- CH species from the C jaws are only pumped by ion pumps. One cannot rely on NEG or Ti sublimations for these.
- Special treatments can decrease performance (e.g. 2 μm PVD Ti coating by a factor of 6). If followed by a bake out at 250°C during 24 h, the material will recover the initial outgassing values.
- If the graphite material is operated above room temperature then the outgassing rate increases steeply. Outgassing rates are increased about tenfold for a 50°C increase of jaw temperature. The jaw temperature should therefore be kept below 50°C.
- A pressure rise by 4 orders of magnitude is expected in the case of an abnormal beam impact (temperature increase to 1050°C) .
- Recovery following dump errors is good with 3 orders of magnitude in vacuum pressure recovered after 1.5 hours. This is short enough to not impose any delays for the refilling of the LHC.

The vacuum studies show that graphite-based jaws are compatible with the LHC vacuum. The outgassing rates of the C jaws of the collimators will be optimized by material and heat treatment under vacuum, an in-situ bake-out and a proper shape design. A survey in the SPS close to the graphite dump revealed no signs of dust and there is no indication that graphite dust may be a problem for the LHC. The magnitude and possible effects of a local electron cloud are being studied.

Impedance implications (resistivity, coating)

Graphite materials have a relatively high resistivity, ranging from 7 $\mu\Omega$m to about 30 $\mu\Omega$m. This results in significant contributions to the LHC impedance from the collimators. In order to minimize impedance it is crucial to select the graphite material with the lowest possible resistivity, if at all possible. A market survey and measurements are ongoing. A thin 1 μm coating of copper might be placed on all graphite collimators, if it can be shown that this coating will adhere reasonably well and will not damage the graphite jaw in case of abnormal beam impact.

18.5.3 Mechanical collimator design

The mechanical design of collimators that can withstand the high intensity LHC beam is challenging. Collimators do not only need to be very robust but at the same time quite long (high energy protons) and very precise (small collimation gaps). The functional requirements for TCP and TCSG collimators are summarized in Table 18.10 [56]. The small minimum gap size of 0.5 mm and the small beam size at the collimators (200 μm rms) implies tight mechanical tolerances. These are relaxed for initial running. The numbers quoted refer to nominal running. Achieving these tolerances would in principle allow closing the TCP and TCSG collimators of phase 1 to 6 σ and 7 σ. For beam-based alignment the jaws must be remotely movable with good precision. Reproducibility of settings is crucial in order to avoid lengthy re-optimizations. The absolute opening of the collimator gap is safety-critical and must be known at all times with good accuracy. A movement orthogonal to the collimation plane allows provision of spare surface, e.g. after coating has been locally damaged by the beam.

Technical concept

The present technical concept (see Figure 18.12) is the result of the analysis of a wide spectrum of options and alternatives [57]; the guiding principle for the mechanical design has been the use and optimization of proven technologies, mainly drawn from LEP collimator experience [58]. However, due to the unprecedented

Table 18.10: Functional requirements for the TCP and TCSG type collimators. The orientation of objects with one or two parallel jaws is horizontal (X), vertical (Y), or close to 45 degree (S). The required degrees of freedom (DOF) for jaw movements are listed.

Parameter	**Unit**	**TCP**	**TCSG**
Azimuthal orientation		X, Y, S	various
Jaw material		C or C-C	C or C-C
Jaw length	cm	20	100
Jaw tapering	cm	2×10	2×10
Jaw dimensions	mm^2	65×25	65×25
Jaw coating		0-1 μm Cu	0-1 μm Cu
Jaw resistivity	$\mu\Omega$m	minimal	minimal
Surface roughness	μm	≤ 1	≤ 1.6
Surface flatness	μm	25	25
Heat load (peak)	kW	1.5	34
Heat load (continuous)	kW	1.5	7
Max. operational temperature	°C	50	50
Outbaking temperature	°C	250	250
Maximum full gap	mm	60	60
Minimum full gap	mm	0.5	0.5
Knowledge of gap	μm	50	50
Jaw position control	μm	≤ 10	≤ 10
Control jaw-beam angle	μrad	≤ 15	≤ 15
Reproducibility of setting	μm	20	20
DOF movement (hor. collimator)		X, X', Y	X, X', Y
DOF movement (vert. collimator)		Y, Y', X	Y, Y', X
Positional installation accuracy	μm	100	100
Angular installation accuracy	μrad	150	150

specification, it was also necessary to make use of innovative technologies and novel materials, such as Carbon/Carbon composites. The main technical features of the LHC secondary collimators are:

1. An internal alignment system allowing both lateral displacement and angular adjustment.
2. A jaw clamping system to ensure good thermal conductance and free thermal expansion.
3. An efficient cooling system.
4. A precise actuation system including a semi-automatic mechanical return and a misalignment prevention device.
5. A plug-in external alignment system, allowing a quick and simple positioning of the collimator assembly in the machine.
6. A motorization and a control set.

The system is free from the effect of vacuum force.

The jaw assembly design

The design of the jaw assembly was chosen based on the clamping concept: the graphite or C/C jaw is pressed against the copper-made heat exchanger by a steel bar on which a series of springs is acting. The jaw assembly is held together by steel plates (see Figure 18.13). To minimize the thermal path from the hottest spot, where the beam impact takes place, to the cooling pipes, the jaw width has been reduced to an allowable

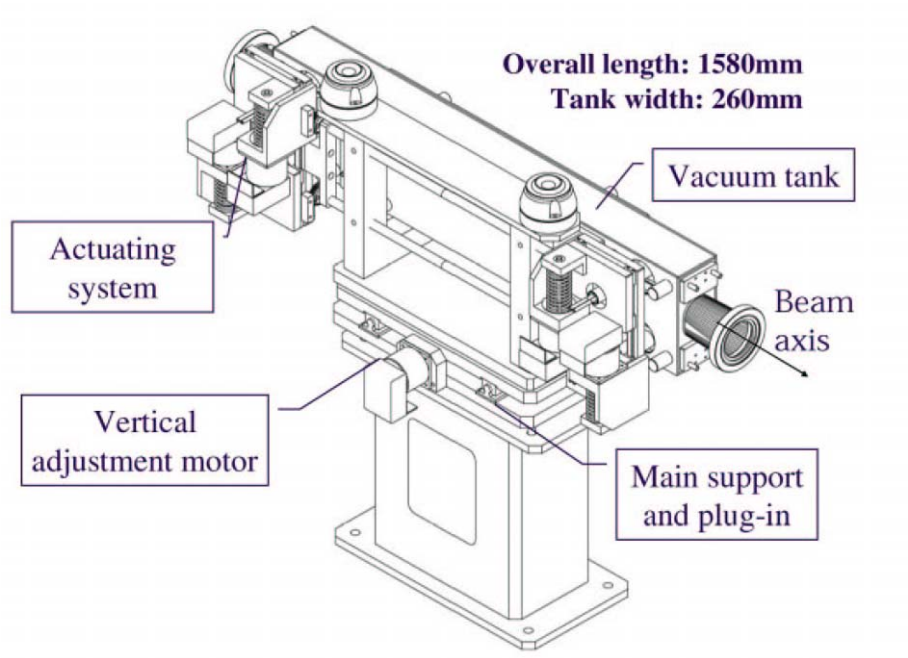

Figure 18.12: General layout and dimensions of the LHC secondary collimator (vertical configuration).

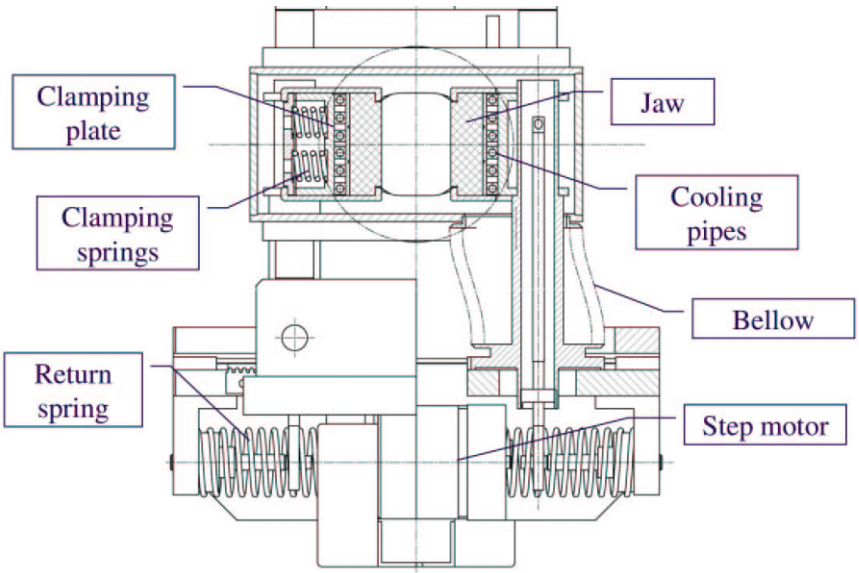

Figure 18.13: Secondary collimator mechanical assembly (cross-section of a horizontal TCSG).

minimum (25 mm), as demanded by preliminary thermo-mechanical analysis. Since the thermal expansion coefficient of copper is three times (or more) larger than graphite's, a fixed joint between the jaw and the copper plate is not possible, if one wants to avoid unacceptable distortions; hence, the contact must allow for relative sliding between the two surfaces. At the same time, to ensure proper heat conduction at the contact interface, a certain pressure has to be applied between these surfaces. The pressure was estimated through a semi-analytical model developed by Fuller and Marotta [59, 60]. A higher pressure leads to better conductance, but, in turn, it means higher mechanical stresses on the jaw; therefore a trade-off had to be found: the nominal pressure on the interface is set to 5 bar. To minimize the effect of differential thermal expansion on the jaw surface precision, the transverse distance from the two supporting axles to the internal reference surface of the jaw has been reduced to 40 mm.

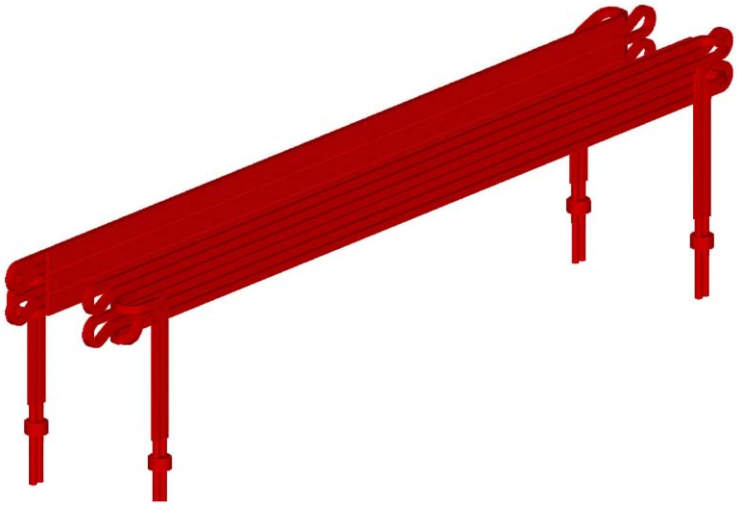

Figure 18.14: Cooling system: the multi-turn cooling pipes and the copper plates.

The cooling system

The heat exchanger is constituted by two OFE-copper pipes per jaw brazed on one side to a copper plate and on the other to a stainless steel bar. Each pipe has three turns to increase the heat exchange (Figure 18.14). To ease the brazing and avoid harmful air traps, the pipe section is square. The inner diameter of the pipes is 6 mm. The measure of the outgassing rates of graphitic materials led to the specification of a maximum operating temperature of 50 °C for the jaw material. This imposes the use of chilled water. To meet such a strict requirement, the coolant temperature must be as low as possible: the assumed inlet temperature is 15°C to limit possible condensation problems (to this regard, a certain margin exists, since temperature could be further reduced to 12 °C). The water flow rate is 5 l/min per pipe, leading to a flow velocity of ≈3 m/s. This value is in fact rather high and might lead to erosion-corrosion problems on the soft copper pipe bends; however it is necessary both to ensure the evacuation of the high heat loads anticipated and to limit the thermally-induced deformations. In any case, the flow rate can be adjusted for each collimator by specific flow-fix valves. A cooling system is also foreseen for the outer surface of the vacuum tank.

Motorization and actuation system

Each jaw is independently actuated by two stepper-motors (Figure 18.15). This allows both lateral displacement (with a nominal stroke of 30 mm plus 5 mm of extra-stroke) and angular adjustment. Excessive tilt of the jaw is prevented by a rack and pinion system which avoids relative deviation between the two axes larger than 2 mm (i.e. 2 mrad). Each motor directly drives, via a roller screw/nut set, a table which allows the precise positioning of the jaw supporting axle. Each table is mounted on anti-friction linear guide-ways. The advancement for each motor step is 10 μm. Vacuum tightness is guaranteed by four bellows which can be bent sideways (not shown). The system is preloaded by a return spring to make the system play-free. The return spring also ensures a semi-automatic back-driving of the jaw in case of motor failure. The position control is guaranteed by the motor encoder and by four linear position sensors. Stops and anti-collision devices for jaw motion are also foreseen.

The vacuum tank and the external alignment system

The vacuum tank has a traditional conception. It is manufactured in AISI 316L stainless steel and mainly electron-beam welded. The structural design is the same for all the collimator configurations (horizontal, vertical or skew). The tank is supported by brackets whose design depends upon the orientation. The whole system is pre-aligned and then placed on a support table via a plug-in system. A stepper motor allows the adjustment

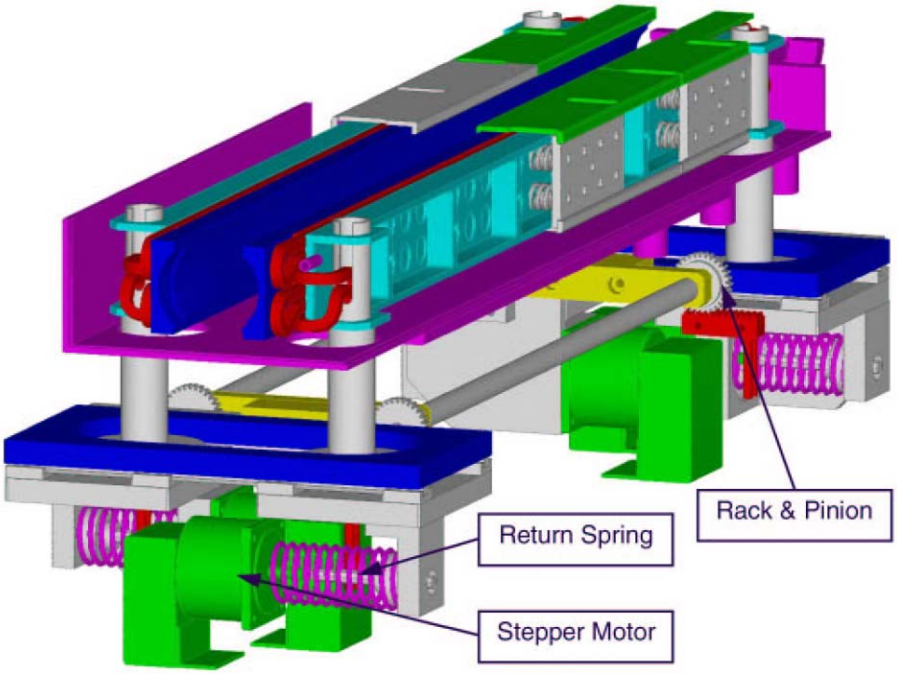

Figure 18.15: Motorization and actuation system.

of the whole assembly by 10 mm in order to move the jaws on the plane of collimation and present a fresher surface in the beam impact area in case the initial impact area is damaged.

Local collimator instrumentation

The collimators will be equipped with sophisticated instrumentation which will provide extensive diagnostics. The main diagnostics information is summarized:

- Position of each motor and jaw support point.
- Independent measurement of collimator gap at both extremities of collimator tank (average gap and angle between the two jaws).
- Independent measurement of one jaw position at both extremities of collimator tank.
- Temperature of each graphite jaw at both of its extremities (start and end).
- Temperature of cooling water at inlet and outlet.
- Signals from various switches (in, out, anti-collision, ...).
- One microphonic sensor per jaw for detection of beam-induced shock waves.
- Flow of cooling water per collimator.

The extensive diagnostics will allow fail-safe setting of collimator gaps, important checks on self-consistency and detection of abnormal beam load conditions.

18.5.4 Tertiary collimators in the experimental insertions (TCT)

The most stringent requirements for the collimation system occur during collisions at 7 TeV when the stored energy is maximal and local aperture restrictions occur at the experimental triplets. In order to protect the

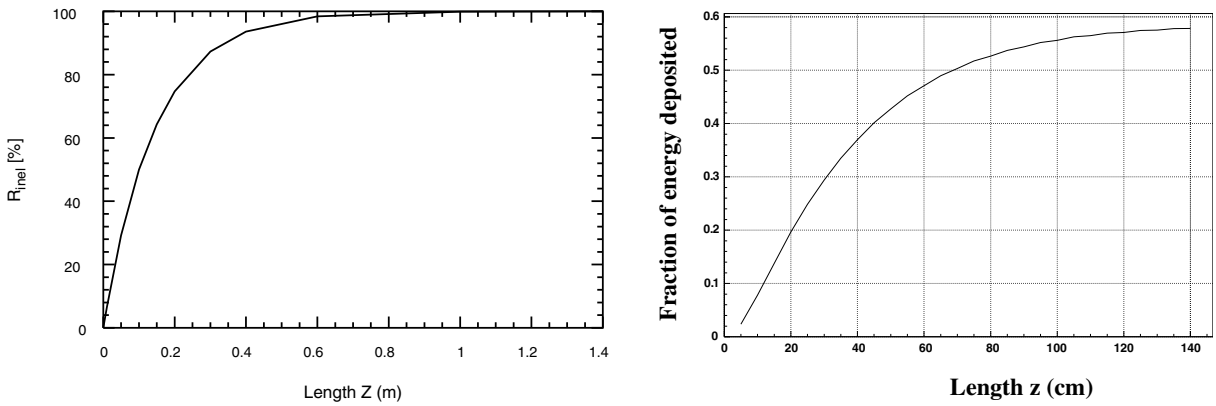

Figure 18.16: Fraction of inelastically interacting protons (left) and fraction of energy deposited (right) in a block of Cu material, plotted as a function of its length. The energy deposition results include the full proton-induced cascade.

triplets in case of the unlikely event that mis-kicked beams escape the protection systems, it is useful to install local protection. In addition, tertiary collimators can help to fulfill the efficiency requirements by providing a local cleaning stage at the location where it is needed. Local cleaning is highly efficient because global changes of beam parameters (orbit, beta beat) do not perturb the local shadow.

The tertiary collimators are presently foreseen close to D1 on each side of the four experimental insertions. Their jaws will be made out of high-Z material. The tertiary halo will be intercepted and diluted, such that less energy reaches the super-conducting triplet magnets. Peaks in tertiary halo (e.g. due to transient drops in beam lifetime) are suppressed and triplet quenches are avoided, even though some background spikes could be expected in the experiments. It is important to realize that these background spikes are the price paid for preventing triplet quenches which would otherwise terminate the physics fill. With tertiary collimators the physics fill can be continued after stable conditions have been restored (perturbations can be as short as a few seconds or minutes). It is expected that significant gains can be made in uptime and integrated luminosity production. If the tertiary collimators generate unforeseen problems they can be moved out from the beam.

In total 16 tertiary triplet collimators will be installed, each made out of copper and with a length of 1.0 m. From Figure 18.16 it is seen that almost all protons in the tertiary halo will interact inelastically and more than 50% of the energy lost stays in the copper block. Therefore the halo-induced heat load in the triplet will be reduced by at least a factor 2 (gaining in effective efficiency). In addition, the tertiary collimators add significant flexibility to the system. For example, one could optimize beam-induced background in the experiments versus luminosity.

The tertiary collimators offer important additional protection against beam losses, in particular for operation at 7 TeV with low beta function at the IP and large beta function in the triplet:

1. In case of abnormal beam dump, the maximum excursion of bunches in the triplet depends on many parameters, such as the orbit at the TCDQ, the orbit at the triplet, etc. An orbit offset of only 1.5 σ at the TCDQ (0.5 σ is the specified tolerance) could result in an impact of one 7 TeV bunch at the superconducting magnets in the triplet. The setting of the tertiary collimators would be such that they shadow the superconducting coils of the triplet magnets. Particle loss would be restricted to the collimator which can be replaced more easily.

2. A failure that leads to an orbit distortion or emittance growth would first result in beam losses at the collimators. Normally, beam loss monitors would detect the losses and request a beam dump. If the beam was not dumped, the showered beam would touch the triplet aperture a short time later and possibly quench or even damage the magnets. With the aperture restriction of the tertiary collimators, close-by beam loss monitors would request a beam dump and therefore ensure some redundancy in the protection.

18.5.5 Additional collimators, absorbers and scrapers

Scrapers (TCSP)

Scraping of proton beams is an important accelerator technique. It is often used for diagnostics purposes, control of background, or to avoid peaks in loss rate. The LHC primary collimators are specified for a minimum opening of 5 σ (about $\pm$ 1 mm). They are crucial for beam cleaning and should not be used for other purposes. It has therefore been decided to include 6 dedicated scrapers (horizontal, vertical, momentum for each beam) into the LHC design and they will be located at the corresponding primary collimators. Material, length, and detailed design of the LHC scrapers remain to be decided. Scrapers are foreseen to be installed for phase 1 of LHC collimation.

Fixed absorbers

The collimators absorb only a small fraction of the energy from the lost protons (on the order of a few %). Particle showers exit from the collimator jaws and carry the lost energy downstream. In order to avoid quenches or excessive heating, the particle cascades must be intercepted by additional fixed absorbers downstream of the collimators. Detailed shower calculations will be performed in order to decide the length, location, and eventual cooling requirements for fixed absorbers. Absorbers will be required for phase 1 of LHC collimation.

Collimators for collision debris (TCLP)

The movable TCLP collimators are used to capture part of the debris from the p-p interactions at the experimental insertions in IR1 and IR5. They will be made out of 1 m long copper jaws and can be installed in two batches of 4 components in phase 1 and phase 3. The detailed design remains to be decided.

Injection collimators (TCLI)

Special TCLI collimators are part of the protection system for LHC injection. These movable devices complement the protection from the TDI device (see Chapter 16) and will intercept mis-kicked beam in IR2 and IR8. A detailed design remains to be decided. TCLI collimators are required for phase 1 of LHC collimation.

18.6 PERFORMANCE REACH WITH PHASE 1 COLLIMATION AND BEYOND

The relevant performance measure of the LHC collimation system is the beam loss rate $R_{\text{sc}}(s)$ in any superconducting magnet of the LHC ring. This maximum loss rate should be below the quench limit $R_q(s)$ and is a function of the cleaning inefficiency $\eta_c(a_c, n_1, n_2, n_3)$ (see Equation 18.3), the minimum beam lifetime at the collimators τ_{min}, the total beam population N_{tot} and some aperture distribution map $A_{\text{dis}}(s, x_0, x_0', y_0, y_0', \delta_0, s_0)$:

$$R_{\text{sc}} \approx \eta_c(a_c, n_1, n_2, n_3) \cdot \frac{N_{\text{tot}}}{\tau_{\text{min}}} \cdot A_{\text{dis}}(s, x_0, x_0', y_0, y_0', \delta_0, s_0) \tag{18.6}$$

The aperture distribution map A_{dis} is a particularly complicated function that depends on the collimator location s_0 where the particle escaped, the particle coordinates (offset in phase space) and the detailed aperture model between the escape location s_0 and the observation point s. Though it is sometimes approximated by the inverse of a so-called dilution length L_{dil}, a reliable determination requires full tracking studies with a detailed aperture model, including aperture imperfections and additional absorbers. These studies are presently not advanced enough to predict local beam loss rate $R_{\text{sc}}(s)$ at the 10^{-5} level of primary beam losses ($10^{-8} - 10^{-9}$ level of totally stored intensity).

Even though detailed performance estimates are not yet possible, it is hoped that the design goals for cleaning efficiency can be met. The collimation system is designed to support up to 40% of design intensity with nominal β^* in phase 1. The phase 2 collimation system should allow nominal and possibly even ultimate running conditions.

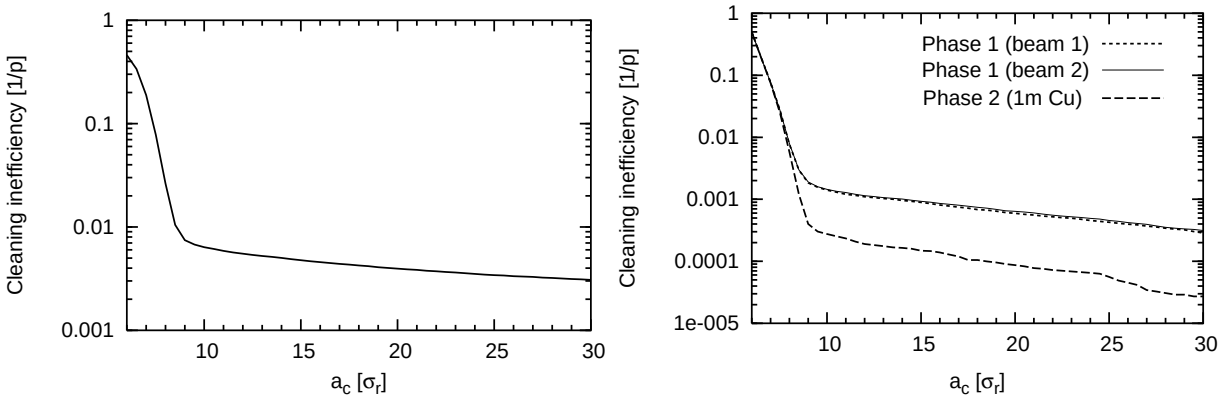

Figure 18.17: Predicted ideal inefficiencies for betatron cleaning at injection (left) and 7 TeV (right) with 6/7 σ settings. The 7 TeV prediction includes phase 1 and phase 2 performance, assuming 1 m Cu jaws for phase 2 collimators.

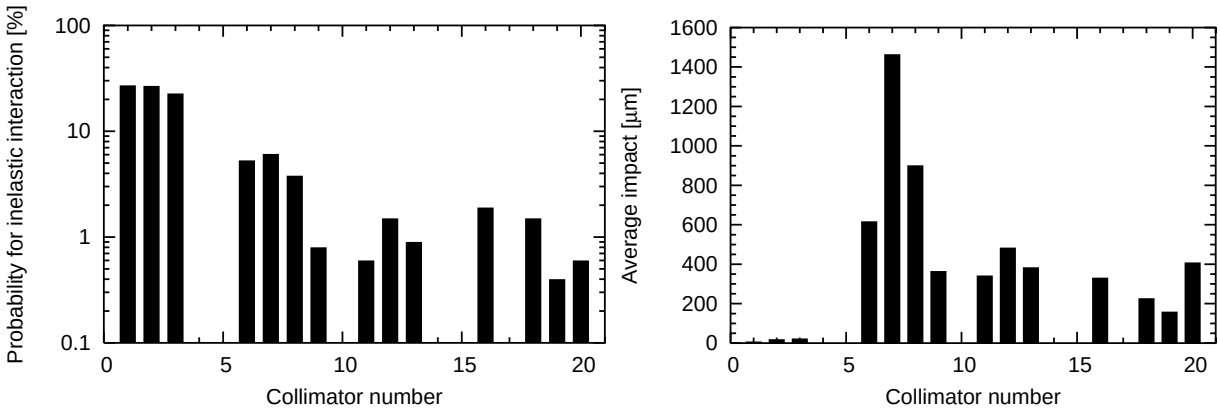

Figure 18.18: Left: Predicted multi-turn probability for inelastic interaction (left) and average impact parameter at the various collimators in the betatron cleaning insertion IR7.

18.6.1 Estimation of ideal cleaning inefficiency

The cleaning inefficiency $\eta_c(a_c, n_1, n_2, n_3)$ (here generalized to include tertiary collimators at a normalized setting of n_3) can be predicted by tracking programs that are also used in the design process of the cleaning insertions. The expected performances at injection and top energy of the betatron cleaning system in IR7 are shown in Figure 18.17. Almost a factor of 10 better inefficiency can be reached with phase 2. It is noted that the results apply for an ideal system with some assumptions on the beam halo (see Figure 18.2) and cannot easily be used to estimate the allowable beam intensity in the LHC ring. Advanced halo tracking in a detailed aperture model must be used for this purpose, as discussed above. Nevertheless it is stated that the design of the collimation systems achieved quite good cleaning inefficiencies that could not be optimized further, given the LHC constraints. The predicted inefficiencies for the ideal betatron collimation at 7 TeV are as low as 11×10^{-4} for phase 1 and 2×10^{-4} for phase 2. The corresponding maximum amplitudes of the on-momentum secondary halo were independently estimated to be 9.3 σ radially and 7.3 σ and 7.4 σ in the horizontal and vertical directions.

The tracking studies provide predictions on other important aspects. Figure 18.18 shows the calculated multi-turn probability for inelastic interaction and the average impact parameter for the various collimators in the betatron cleaning insertion IR7. The locations of inelastic interactions of lost protons is an important input for understanding the loss distribution and activation in IR7. The impact parameter at the secondary collimators (defined as transverse distance between proton impact point and collimator edge) determines important tolerances, e.g. the required surface flatness and allowable angular imperfections.

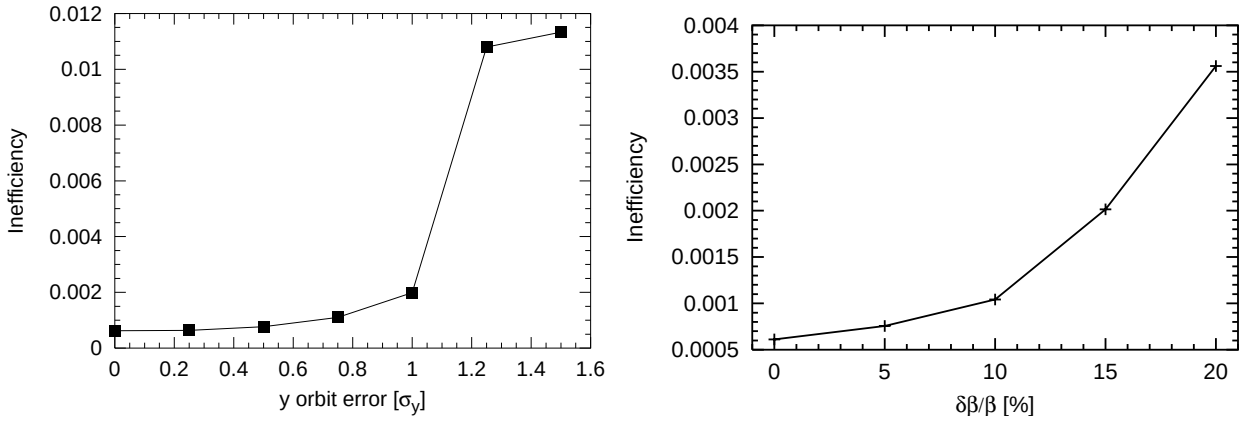

Figure 18.19: Left: Dependence of the collimation inefficiency on an uncontrolled change in vertical orbit (worst phase). Right: Dependence of the collimation inefficiency on an uncontrolled transient beta beat (worst phase).

18.6.2 Collimation tolerances

A complete and consistent study of collimation tolerances remains to be completed and the numbers listed should be used as preliminary estimates only.

The proper functioning of the LHC collimation system depends on the concept of a two stage cleaning process in IR3 and IR7. This implies that the secondary collimators must never become primary collimators. The relative retraction between the two settings is nominally 1 σ, about 1.2 mm at injection and 0.2 mm at top energy. Several effects can change the relative retraction of collimators with respect to the beam orbit. In particular orbit changes and transient changes in beta beat must be avoided. In addition mechanical deformations of the jaws can cause perturbations. The most severe tolerances apply for 7 TeV where the nominal 200 μm relative retraction can be reduced by several possible sources of errors. It is noted that this retraction should not be smaller than about 0.5 σ or 100 μm at 7 TeV. The tolerances for mechanical jaw properties were listed in Table 18.10 for nominal collimation settings (6/7 σ).

Operational tolerances were preliminarily estimated for the 7 TeV nominal collimation settings (6/7σ), each tolerance leading to a 50% increase in cleaning inefficiency [61]. A consistent and combined treatment of all tolerances remains to be completed. The results of studies are illustrated in Figure 18.19. The corresponding tolerances are summarized in Table18.11 for nominal conditions and for an early 7 TeV collimation setting that relaxes operational tolerances. A relaxation of tolerances at 7 TeV is achieved by choosing for example a 3.5 σ retraction between primary and secondary collimators during early collisions (requiring a higher β^* in the range of 1-2 m). The collimation process can thus be made compatible with a natural learning curve in operation and optimization of the LHC. The tertiary collimators provide an additional gain in operational tolerances at 7 TeV which was not included in the numbers listed. It is noted that tolerances at injection cannot be relaxed, except by storing less intensity.

18.6.3 Operational conditions for collimation

The operational set-up of the LHC collimation system for significant intensities can be envisaged only after some pre-requisites have been fulfilled by LHC operation. They are listed in order of importance:

- Design aperture has been established (in particular a maximum beta beat of 20% and a maximum peak orbit of 4 mm must be guaranteed during the LHC beam cycle).
- Nominal beam loss rates have been established (the minimum beam lifetime should not drop below 0.2 h during the full LHC beam cycle).
- Transient changes in orbit and beta beat are under control, fulfilling the collimation injection tolerances (orbit and tune loops have been commissioned).

Table 18.11: Important operational tolerances for collimation, each defined for a 50% increase in cleaning inefficiency (preliminary estimates). Interdependencies between errors are not yet taken into account. The β^* for relaxed conditions depends on the stored intensity and should be in the range of 1-2 m.

Parameter	Tolerances		
	Nominal injection	Collision (nominal)	Collision (relaxed β^*)
(n_1/n_2)	(6/7 σ)	(6/7 σ)	(7/10.5 σ)
Beam size at collimators	$\approx$ 1.2 mm	$\approx$ 0.2 mm	$\approx$ 0.2 mm
Orbit change	0.6 σ $\approx$ 0.7 mm	0.6 σ $\approx$ 0.12 mm	2.0 σ $\approx$ 0.4 mm
Transient beta beat	8%	8%	80%
Collinearity beam-jaw	50 μrad	50 μrad	75 μrad

The margin gained by running with lower intensities would be used for bringing up cleaning efficiency from an initially sub-optimal to a fully optimized situation.

The collimation system will be operationally characterized by the achieved cleaning efficiency and the induced impedance. The operational conditions of the LHC must be adapted accordingly with possible consequences on the stored beam intensity and the β^* in the experimental insertions. Possible operational measures to help collimation performance are described:

- Decrease of stored intensity as a measure to adapt to limited cleaning efficiency or to reduce the effects of collimator induced impedance. For impedance it is important to carefully consider reductions in bunch intensity or number of bunches.

- Increase of β^* at top energy as a measure to adapt to limited cleaning efficiency or to increase the collimator gaps. Wider collimator gaps are helpful to relax operational tolerances (improve collimation efficiency) or to reduce the effects of collimator induced impedance.

It is expected that impedance limitations become apparent only at 7 TeV if more than about 40% of nominal intensity is stored with a 25 ns bunch spacing (see Chapter 5). A careful trade-off will be required to define the optimal operational strategy with collimation, based on the actually observed limitations in the LHC machine. The tertiary collimators increase the operational flexibility and introduce additional ways of optimizing performance.

18.6.4 Beam-based optimization of collimator settings with Beam Loss Monitors

The set-up and optimization of the collimation system will be done in several beam-based steps, relying on the measurements from Beam Loss Monitors (BLM's) which will be installed near every collimator [24]. Following set-up procedures at other colliders the following logic could apply:

1. Separate beam-based calibration of each collimator: After producing a well-defined cut-off in the beam distribution (e.g. with a scraper), the two ends of each collimator jaw are moved until the beam edge is touched (witnessed by a downstream beam loss signal). This step defines an absolute reference position and angle for each jaw, which is valid for given and hopefully reproducible orbit and optics functions.

2. System set-up: After restoring the reference beam conditions all collimators are set to their target gaps and positions, directly deduced from the absolute reference positions obtained in step 1. The cleaning inefficiency is observed in a few critical BLM's in the downstream areas.

3. Empirical system tuning: The cleaning inefficiency is minimized by empirical tuning on the few relevant BLM's where quenches can occur. The most efficient collimators are optimized first. The optimization is orthogonal if the beam direction is followed. Possible cross-talks between beams can be avoided by single beam optimization.

4. Automatic tuning algorithms: Once some experience has been gained with the collimation system a more advanced automatic tuning algorithm may be envisaged, taking into account collimator response matrices.

The detailed process of set-up and optimization of the collimation system requires further studies and work.

Some effort has already been invested in understanding the BLM response to beam loss in the cleaning insertions. Considering advanced scenarios (all collimators used simultaneously for optimization) it was found that the data recorded near collimators is difficult to use and to interpret. At high energy, the cascade developed in a jaw and in the surrounding material will induce signals in all monitors which are installed nearby and downstream. In order to understand how to use the signals, a preparatory simulation was done with MARS, which develops cascades into the entire momentum cleaning section, including 7 collimators and BLM monitors, vacuum chambers, magnets with their field, tunnel, ground, etc [62]. A primary impact map was generated. The partial fluences as issued from every collimator were recorded at each monitor, allowing a matrix to be built which allows the computation of the normalized rate s_i at every monitor as a function of the primary rate r_i at each collimator. For nominal working condition at injection energy, for $\vec{s} = \mathbf{M}\,\vec{r}$, $\mathbf{M}$ is equal to

$$M = \begin{bmatrix} .0178 & .0 & .0 & .0 & .0 & .0 & .0 \\ .4662 & 1.19 & .0 & .0 & .0 & .0 & .0 \\ .0268 & .0291 & 1.081 & .0004 & .0 & .0 & .0 \\ .0432 & .0389 & 1.085 & 1.044 & .0 & .0 & .0 \\ .0079 & .0036 & .138 & .3245 & .9891 & .0 & .0 \\ .0036 & .0017 & .03858 & .1187 & .513 & .9848 & .0 \\ .0012 & .0007 & .0099 & .0349 & .1642 & .5093 & .9445 \end{bmatrix}. \tag{18.7}$$

Further work will include a variation of the jaw depth n_i one by one, in order to map $\mathbf{M}$ as a function of $\vec{n}$. $\mathbf{M}$ may be constructed by sending a pilot bunch on each jaw sequentially. With the high value of many non-diagonal terms in $\mathbf{M}$, it is not yet sure that unambiguous calculations of the loss rate on every collimator can be deduced with this approach. This will only become an issue once it is tried to tune many collimator settings at once, e.g. trying to speed up optimization procedures after a few years of operation. Initial one-by-one studies will result in easily understandable response matrices.

REFERENCES

[1] R. Assmann. Proc. Chamonix 2003. CERN-AB-2003-008 ADM.

[2] J.B. Jeanneret, D. Leroy, L. Oberli and T. Trenkler. LHC Project Report 44 (1996).

[3] R. Assmann, F. Schmidt, F. Zimmermann, M.P. Zorzano. LHC-PROJECT-REPORT-592. EPAC02.

[4] L. Burnod and J.B. Jeanneret. CERN-SL-91-39-EA. LHC-Note-167 (1991).

[5] P. Bryant and E. Klein. CERN-SL-92-40-AP (1992).

[6] P. Bryant. CERN-SL-AP-92-024 (1992).

[7] P. Bryant et al. CERN-SL-AP-93-015 (1993).

[8] P. Bryant and E. Klein. SL-Note-93-29-AP (1993).

[9] T. Risselada. SL Note 95-32 AP. LHC Note 317 (1995).

[10] J.B. Jeanneret, "Optics of a two-stage collimation system". CERN-LHC-Project-Report-243 (1998).

[11] I.L. Azhgirey, I.S. Baishev, N. Catalan-Lasheras, J.B. Jeanneret, "Cascade Simulations for the LHC Betatron Cleaning Insertion". LHC-Project-Report-184 (1998).

[12] N. Catalan-Lasheras, G. Ferioli, J.B. Jeanneret, R. Jung, D. Kaltchev, T. Trenkler. LHC-Project-Report-156 (1997).

[13] R. Assmann et al. PAC03. CERN-LHC-Project-Report-640 (2003).

[14] R. Assmann, C. Fischer, J.B. Jeanneret, R. Schmidt. LHC-PROJECT-NOTE-282 (2002).

[15] P. Sievers et al. Proc. Chamonix 2003. CERN-AB-2003-008 ADM.

[16] R. Assmann, B. Goddard, E. Vossenberg, E. Weisse. LHC-Project Note 293 (2002).

[17] R. Assmann et al. LHC-PROJECT-REPORT-599. EPAC02.

[18] M. Hayes et al. EPAC02. CERN-LHC-Project-Report-589.

[19] R. Assmann et al. LHC-PROJECT-NOTE-277 (2002).

[20] T. Risselada. SL Note 92-16 AP. 1992.

[21] R. Schmidt. Proc. Chamonix 2003. CERN-AB-2003-008 ADM.

[22] R. Schmidt et al. Proc. HALO03. CERN-LHC-Project-Report-665 (2003).

[23] B. Dehning. Proc. Chamonix 2003. CERN-AB-2003-008 ADM.

[24] J.B.Jeanneret et al., CERN LHC-BLM-ES-0001.00 rev 1.1, EDMS doc 328146, 2003.

[25] L. Burnod and J.B. Jeanneret. AC/DI/FA/Note 92-05 (1992).

[26] J. Uythoven. Reported at the 24^{th} meeting of the Collimation WG (http://www.cern.ch/lhc-collimation).

[27] H. Burkhardt. Proc. Chamonix 2003. CERN-AB-2003-008 ADM.

[28] H. Burkhardt. Reported at the 27^{th} meeting of the Collimation WG (http://www.cern.ch/lhc-collimation).

[29] B. Goddard. Reported at the 23^{rd} meeting of the Collimation WG (http://www.cern.ch/lhc-collimation).

[30] T.Trenkler, J.B.Jeanneret, CERN SL/Note94-105(AP), 1994.

[31] F. Schmidt, "SixTrack, User's Reference Manual", CERN SL/94-56 (AP).

[32] I. Baichev, D. Kaltchev, *Implementation in Dimad of a new Collimator Element (STRUCT module)*, TRIUMF Report (in preparation)

[33] R.V.Servranckx, *User's Guide to the Program Dimad*, TRIUMF Design Note, TRI-DN-93-K233, (1993).

[34] J.B. Jeanneret, SL/Note 92-56 (EA).

[35] I. Baishev et al., CERN LPR 309 (1999).

[36] J.B.Jeanneret, CERN/SL/92-44(EA).

[37] E. Chapochnikova. Proc. Chamonix 2003. CERN-AB-2003-008 ADM.

[38] E. Chapochnikova, S. Fartoukh and J.B. Jeanneret, CERN LPN, to be issued 2003.

[39] A.I. Drozhdin et al., Fermilab Project Note FN-0724,2002.

[40] J.B. Jeanneret, Phys. Rev. ST Accel. and Beams, **1**, 081001, December 1998.

[41] T. Risselada. SL Note 95-67 AP (1995).

[42] I. Ajguirei, I. Baichev, J.B. Jeanneret, I.A. Kourotchkine and G.R. Stevenson. CERN-LHC-Project-Note-263 (2001).

[43] Instruction de securite, Safety instructions, CERN IS 23 (Rev. 2), Edms 335745.

[44] R. Assmann. Proposal to the AB LHC Technical Committee (LTC) on June 25^{th}, 2003.

[45] R. Assmann et al. PAC03. CERN-LHC-Project-Report-639 (2003).

[46] M. Brugger. Proposal to the AB LHC Technical Committee (LTC) on June 25th, 2003.

[47] M. Brugger, S. Roesler, "Remanent Dose Rates in the LHC Beam Cleaning Insertions", CERN-TIS-2003-026-RP-TN, 2003.

[48] O. Aberle. May 2003.

[49] M. Brugger, S. Roesler, "Accumulated Doses during Interventions on the Vacuum System in the LHC Beam Cleaning Insertions", CERN-TIS-2003-027-RP-TN, 2003.

[50] O. Aberle. Proposal to the AB LHC Technical Committee (LTC) on June 25^{th}, 2003.

[51] F. Ruggiero. Proposal to the AB LHC Technical Committee (LTC) on June 25^{th}, 2003.

[52] A. Fasso, A. Ferrari, J. Ranft, P.R. Sala. Proc. of the Int. Conf. Monte-Carlo 2000, Lisbon, Portugal, Oct. 23-26, 2000, p. 955, Springer-Verlag Berlin Heidelberg (2001).

[53] V. Vlachoudis. Proposal to the AB LHC Technical Committee (LTC) on June 25^{th}, 2003.

[54] M. Zyczkowski, Combined Loadings in the Theory of Plasticity, Chapter 11.

[55] M. Jimenez. Proposal to the AB LHC Technical Committee (LTC) on June 25^{th}, 2003.

[56] O. Aberle and R. Assmann. July 2003.

[57] A. Bertarelli and R. Perret. Proc. Chamonix 2004.

[58] R. Perret, Note Technique MT-ESI/94-3, 1994.

[59] E. Marotta, S. Mazzucca, J. Norley. Electronic Cooling, 8 (2003) 3.

[60] J.J. Fuller, E. Marotta. Journal of Thermophysics and Heat Transfer, 15 (2001) 2.

[61] R.W. Assmann, J.B. Jeanneret, D. Kaltchev. EPAC02. LHC-PROJECT-REPORT-598 (2002).

[62] I. Ajguirei, I.S. Baichev, J.B. Jeanneret and I.A. Kourotchkine, CERN LPN, to be issued, 2003.